



Journal of Difference Equations and Applications

ISSN: 1023-6198 (Print) 1563-5120 (Online) Journal homepage: <http://www.tandfonline.com/loi/gdea20>

Complex dynamics of a discrete predator-prey model with the prey subject to the Allee effect

Daiyong Wu & Hongyong Zhao

To cite this article: Daiyong Wu & Hongyong Zhao (2017) Complex dynamics of a discrete predator-prey model with the prey subject to the Allee effect, *Journal of Difference Equations and Applications*, 23:11, 1765-1806, DOI: [10.1080/10236198.2017.1367389](https://doi.org/10.1080/10236198.2017.1367389)

To link to this article: <https://doi.org/10.1080/10236198.2017.1367389>



Published online: 24 Aug 2017.



Submit your article to this journal



Article views: 80



View related articles



View Crossmark data



Complex dynamics of a discrete predator–prey model with the prey subject to the Allee effect

Daiyong Wu^{a,b} and Hongyong Zhao^a

^aDepartment of Mathematics, School of Sciences, Nanjing University of Aeronautics and Astronautics, Nanjing, China; ^bDepartment of Mathematics, Anqing Normal University, Anqing, China

ABSTRACT

In this paper, complex dynamics of the discrete predator–prey model with the prey subject to the Allee effect are investigated in detail. Firstly, when the prey intrinsic growth rate is not large, the basins of attraction of the equilibrium points of the single population model are given. Secondly, rigorous results on the existence and stability of the equilibrium points of the model are derived, especially, by analyzing the higher order terms, we obtain that the non-hyperbolic extinction equilibrium point is locally asymptotically stable. The existences and bifurcation directions for the flip bifurcation, the Neimark–Sacker bifurcation and codimension-two bifurcations with 1:2 resonance are derived by using the center manifold theorem and the bifurcation theory. We derive that the model only exhibits a supercritical flip bifurcation and it is possible for the model to exhibit a supercritical or subcritical Neimark–Sacker bifurcation at the larger positive equilibrium point. Chaos in the sense of Marotto is proved by analytical methods. Finally, numerical simulations including bifurcation diagrams, phase portraits, sensitivity dependence on the initial values, Lyapunov exponents display new and rich dynamical behaviour. The analytic results and numerical simulations demonstrate that the Allee effect plays a very important role for dynamical behaviour.

ARTICLE HISTORY

Received 27 October 2016
Accepted 3 August 2017

KEYWORDS

Allee effect; predator–prey model; flip bifurcation; Neimark–Sacker bifurcation; codimension-two bifurcation; Marotto’s Chaos

AMS SUBJECT CLASSIFICATIONS

92D25; 39A30

1. Introduction

The Allee effect has been formalized and initiated by the work of the biologist W. C. Allee in the early twentieth century [1]. Allee demonstrated this effect with real aggregation experiments, contradicting the paradigm of the classical logistic growth model. It is well known that a population has a slow growth in the beginning, a phase of rapid acceleration and finally a phase of stationary growth in the classical logistic growth model. Allee observed that such growth may exist but there may be also the extinction of the species in a small population size. The Allee effect may be caused by a variety of mechanisms operating in small population sizes, including difficulties in finding mates, reduced foraging efficiency in social animals, lessened defenses against predators, and reduced reproductive success in cooperative breeders [3,5,11,29]. In fact, these mechanisms can be roughly divided into two categories, those that affect reproduction rate and those that affect survival rate. Some

experimental evidences of Allee effects have been reported in many natural populations including plants [15,16], insects [20], marine invertebrates [34], bacteria [33], mammals and birds [10,12].

It is now well understood that the Allee effect can greatly increase the likelihood of extinctions. Therefore, the study of the Allee effect is important to conservation biology. Many expressions have been used in the literature to describe the Allee effect [4,6,17–19], most of them proposed phenomenologically, of which the following Allee effect model [5,10], with non-overlapping generations, is the most frequently used

$$x_{n+1} = x_n + rx_n \left(1 - \frac{x_n}{K}\right) \left(\frac{x_n}{K} - \frac{A}{K}\right), \quad (1)$$

where r denotes the intrinsic growth rate; K denotes the carrying capacity; A denotes the Allee threshold; $r \left(1 - \frac{x_n}{K}\right) \left(\frac{x_n}{K} - \frac{A}{K}\right)$ denotes the density-dependent per capita growth rate, which is negative/positive for decreasing/increasing populations. When $0 < A < K$, the population growth rate decreases if the population size is below this threshold A and this case refers to as a strong Allee effect.

Among various mathematical models, predator-prey models, which have attracted great attention in the past decade, play a vital role in the population dynamics. Such models governed by both difference equations and differential equations may be found in [10,26, 35] and the references cited therein. However, not much work have addressed the Allee effect with focus on the dynamic behaviour of discrete predator-prey models. Celik and Duman [6] provided the conditions of the stability for the following discrete predator-prey model without the Allee effect

$$\begin{cases} x_{n+1} = x_n + rx_n(1 - x_n) - ax_n y_n, \\ y_{n+1} = y_n + ay_n(x_n - y_n), \end{cases} \quad (2)$$

where x_n and y_n denote the densities of prey and predator populations at time n ; r and a are positive constants. Here, $x_n(1 + r(1 - x_n))$ represents the rate of the increase of the prey population in the absence of predator while $ax_n y_n$ represents the rate of decrease due to predation, where the parameter a is the predator parameter. $y_n(1 + a(x_n - y_n))$ represents the variant of the predator density with respect to the prey population. ay_n^2 is the density dependent term. One can notice that if the predator density disappears in the model (2), then the prey density satisfies the classical discrete logistic model. Yuan and Yang [38] discussed the codimension-one bifurcations and codimension-two bifurcation associated with resonance 1:2 for the model (2). Celik and Duman further researched the stability of the positive equilibrium point of the model (2) with the impact of the Allee effect on the prey population as follows

$$\begin{cases} x_{n+1} = x_n + rx_n(1 - x_n) \frac{x_n}{u + x_n} - ax_n y_n, \\ y_{n+1} = y_n + ay_n(x_n - y_n), \end{cases} \quad (3)$$

where $\frac{x_n}{u+x_n}$ denotes the Allee effect function and u is the Allee effect constant. This Allee effect function bases mainly on the difficulties in finding mates [3,5,29]. Chen, Fu and Jing [7] further discussed the codimension-one bifurcation of the positive equilibrium point

of the model (3). Zhang, Zhang and Zhao [39] took $x_n - c$ as the Allee effect function which occurs on the prey population and discussed the codimension-one bifurcation of the positive equilibrium point of the model as follows

$$\begin{cases} x_{n+1} = x_n + rx_n(1 - x_n)(x_n - c) - ax_ny_n, \\ y_{n+1} = y_n + bx_ny_n - dy_n. \end{cases} \quad (4)$$

Cheng and Cao [8] took also $x_n - c$ as the Allee effect function and discussed the codimension-one bifurcation of a discrete-time ratio-dependent predator-prey model with the prey population subject to the Allee effect. In addition, detailed investigations relating the Allee effect may be found in the papers [9,18,36].

In this paper, we consider discrete predator-prey model with the prey subject to the Allee effect as follows

$$\begin{cases} x_{n+1} = x_n + rx_n(1 - x_n)(x_n - c) - ax_ny_n, \\ y_{n+1} = y_n + ay_n(x_n - y_n), \end{cases} \quad (5)$$

where r and a are positive constants. c is the Allee threshold and $0 < c < 1$ represents strong Allee effects. In the following, we call also the model (5) as the map (5).

On the other hand, for discrete models, the existence and direction of bifurcations, especially codimension-two bifurcations, are research focuses (see [7,8,23,24,36,39]). Moreover, bifurcation behaviours may lead to chaos.

This paper is organized as follows: In Section 2, the stability and the basins of attraction of the equilibrium points of the single prey population are analyzed. In Section 3, the existence and stability of the non-negative equilibrium points of the predator-prey system with the prey subject to the Allee effect are obtained. In Section 4, conditions on the existence and direction of codimension-one bifurcations including the flip bifurcation and the Neimark-Sacker bifurcation are given. In Section 5, the existences and the truncated normal forms for codimension-two bifurcations with resonance 1:2 are discussed. In Section 6, by analytical methods, conditions on the existence of Marotto's chaos are derived. In Section 7, numerical simulations are presented to verify the theoretical analysis and to exhibit other complex dynamics. Finally, a brief discussion of our mathematical and ecological findings is given in concluding section.

2. The prey population

In the absence of the predator population, the model (5) reduces to a one-dimensional model

$$x_{n+1} = x_n + rx_n(1 - x_n)(x_n - c). \quad (6)$$

Clearly, the model (6) have three equilibrium points: 0, c and 1. Next we discuss the stability of the three equilibrium points. Denote the map

$$f(x) = x + rx(1 - x)(x - c). \quad (7)$$

Then

$$f'(x) = -3rx^2 + 2r(c+1)x + 1 - rc. \quad (8)$$

Notice that

$$(2r(c+1))^2 + 12r(1-rc) = 4r^2(c^2 - c + 1) + 12r > 0.$$

One can obtain that $f'(x)$ have two zero points

$$\tilde{x} = \frac{c+1}{3} - \frac{\sqrt{r^2(1+c)^2 + 3r(1-rc)}}{3r}, \quad \hat{x} = \frac{c+1}{3} + \frac{\sqrt{r^2(1+c)^2 + 3r(1-rc)}}{3r}.$$

Furthermore, if $rc \leq 1$, then $\hat{x} > 0 \geq \tilde{x}$, and $f(x)$ has unique positive zero point

$$\eta = \frac{c+1}{2} + \frac{1}{2}\sqrt{(c+1)^2 + 4\left(\frac{1}{r} - c\right)}$$

and $f(x)$ is increasing on $[0, \hat{x}]$ and decreasing on $[\hat{x}, \infty)$; If $rc > 1$, then $\hat{x} > \tilde{x} > 0$, and $f(x)$ have two positive zero points η and

$$\tilde{\eta} = \frac{c+1}{2} - \frac{1}{2}\sqrt{(c+1)^2 + 4\left(\frac{1}{r} - c\right)},$$

and $f(x)$ is decreasing on $[0, \tilde{x}] \cup [\hat{x}, \infty)$ and increasing on $[\tilde{x}, \hat{x}]$. One can notice that if $x \in (0, \tilde{x})$, then $f(x) < 0$. Let

$$x_c = \frac{1}{2} + \frac{1}{2}\sqrt{1 + \frac{4}{r}},$$

then $f(x_c) = c$ and $x_c > \hat{x} > c$. When $r \leq \frac{1}{1-c}$, i.e. $\hat{x} \geq 1$, we have $f(\hat{x}) \leq \hat{x} < x_c$. When $r > \frac{1}{1-c}$, i.e. $c < \hat{x} < 1$, by simple computation, we can obtain that

$$\frac{df(\hat{x})}{dr} = \hat{x}(1-\hat{x})(\hat{x}-c) > 0$$

which implies that $f(\hat{x})$ strictly increases on r . Moreover,

$$\frac{dx_c}{dr} = -\frac{1}{r^2} \left(1 + \frac{4}{r}\right)^{-\frac{1}{2}} < 0, \quad \frac{d\eta}{dr} = -\frac{1}{r^2} \left((c+1)^2 + 4\left(\frac{1}{r} - c\right)\right)^{-\frac{1}{2}} < 0$$

which imply that x_c and η strictly decrease on r . These show that there exist unique \hat{r} and \tilde{r} such that $f(\hat{x}) = x_c$ when $r = \hat{r}$ and $f(\hat{x}) = \eta$ when $r = \tilde{r}$, respectively.

Considering the ecological meaning, we always assume that $r \leq \min\{\frac{1}{c}, \tilde{r}\}$ in this section. Take the initial condition $x_0 \in [0, \eta]$. It is easy to see that $(0, \eta)$ is positively invariant for the map f . Substituting 0, c , 1 to the map f , we can obtain that

$$f'(0) = 1 - rc, f'(c) = 1 + rc(1-c), f'(1) = 1 + r(c-1), \quad (9)$$

respectively. Under the condition $rc \leq 1$, $0 \leq f'(0) < 1$. Hence, the equilibrium point 0 is locally asymptotically stable. Since $f'(c) > 1$, the equilibrium point c is unstable. The equilibrium point 1 is locally asymptotically stable if $r < \frac{2}{1-c}$ and unstable if $r > \frac{2}{1-c}$.

Denote $r_0 = \frac{2}{1-c}$. If $r = r_0$, then $f'(1) = -1$ and the equilibrium point 1 is non-hyperbolic. Thus there may be the flip bifurcation at the equilibrium point 1 if the

parameters vary in the small neighbourhood of r_0 . We first study the stability of the equilibrium point 1 when $r = r_0$. It follows that

$$f''(x) = -6rx + 2r(c+1), \quad f'''(x) = -6r.$$

Since the Schwarzian derivative of the map f at $x = 1, r = r_0$ is

$$\left[\frac{f'''(x)}{f'(x)} - \frac{3}{2} \left(\frac{f''(x)}{f'(x)} \right)^2 \right] \Big|_{x=1, r=r_0} = \frac{12}{1-c} \left(1 - \frac{2(2-c)^2}{1-c} \right) < 0,$$

by Theorem 1.16 in [14], the equilibrium point 1 is locally asymptotically stable.

In order to prove the flip bifurcation, we apply [21] to verify that the following nondegeneracy conditions are satisfied

$$\left. \frac{\partial^2 f}{\partial x \partial r} \right|_{x=1, r=r_0} \neq 0$$

and

$$\left[\frac{1}{2} \left(\frac{\partial^2 f}{\partial x^2} \right)^2 + \frac{1}{3} \frac{\partial^3 f}{\partial x^3} \right] \Big|_{x=1, r=r_0} \neq 0.$$

A simple computation shows that

$$\left. \frac{\partial^2 f}{\partial x \partial r} \right|_{x=1, r=r_0} = c - 1 \neq 0$$

and

$$\left[\frac{1}{2} \left(\frac{\partial^2 f}{\partial x^2} \right)^2 + \frac{1}{3} \frac{\partial^3 f}{\partial x^3} \right] \Big|_{x=1, r=r_0} = 8 + \frac{12}{1-c} + \frac{8}{(1-c)^2} > 0. \quad (10)$$

Thus, the flip bifurcation occurs at $r = r_0$. Moreover, by the nondegeneracy condition (10), a unique and stable period-two cycle bifurcates from the equilibrium point 1 as r varies and passes through r_0 .

For $x \in [0, \eta]$, $f^0(x)$ denotes x , while $f^{k+1}(x)$ denotes $f(f^k(x))$ for $k = 0, 1, 2, \dots$. In the following, we prove that the map f possesses chaotic behaviour in the sense of Li-Yorke. By the Li-Yorke's Theorem in [25], we need verify that the map f has positive period-3 points $\{\bar{x}_1, \bar{x}_2, \bar{x}_3\}$, i.e.

$$\begin{aligned} G(x) &= \frac{1}{r}(f^3(x) - x) = x(1-x)(x-c) + f(x)(1-f(x))(f(x)-c) \\ &\quad + f^2(x)(1-f^2(x))(f^2(x)-c) \end{aligned}$$

has zero points on (c, x_c) . Then

$$\begin{aligned} G'(x) &= -3x^2 + 2(c+1)x - c + (-3(f(x))^2 + 2(c+1)f(x) - c)f'(x) \\ &\quad + (-3(f^2(x))^2 + 2(c+1)f^2(x) - c)f'(f(x))f'(x) \end{aligned}$$

Table 1. Values of the parameters for the map f having positive period-3 points $\{\bar{x}_1, \bar{x}_2, \bar{x}_3\}$.

r	c	r_0	\hat{x}	$G(\hat{x})$	\bar{x}_1	\bar{x}_2	\bar{x}_3
3.7	0.1	2.222	0.7961	-0.1745	0.4146	0.6971	1.1636
3.6	0.1	2.222	0.8098	-0.1367	0.4265	0.7139	1.1653
4	0.2	2.5	0.8203	-0.1012	0.5613	0.9171	1.1352
4.1	0.2	2.5	0.8092	-0.1323	0.4599	0.7246	1.1538

and

$$G'(c) = c(1 - c)(1 + f'(c) + (f'(c))^2) > 0, G'(1) = (c - 1)(1 + f'(1) + (f'(1))^2).$$

Since $f'(1) < -1$, $G'(1) < 0$ and $\hat{x} < 1$. Notice $G(c) = G(1) = 0$. Thus, if $G(\hat{x}) \leq 0$, then $G(x)$ has zero point on $(c, 1)$, i.e. the map f has positive period-3 points. Notice that

$$\lim_{r \rightarrow \hat{r}} G(\hat{x}) = \hat{x}(1 - \hat{x})(\hat{x} - c) + x_c(1 - x_c)(x_c - c) = \frac{c - \hat{x}}{\hat{r}} < 0. \quad (11)$$

It can obtain from (11) that when r is larger, the map f exist period-3 points. Table 1 shows that the map f exist the positive period-3 points.

Now we summarize below

Theorem 2.1: *The model (6) have three equilibrium points 0, c and 1. The equilibrium point 0 is locally asymptotically stable and c is unstable. The equilibrium point 1 is locally asymptotically stable if $r \leq r_0$ and unstable if $r > r_0$. Moreover, the model (6) undergoes the flip bifurcation at $r = r_0$ and eventually possesses chaotic behaviour in the sense of Li–Yorke as r increases.*

In the following, we discuss the basin of attraction of the equilibrium point. Let $\mathcal{B}(x)$ denote the basin of attraction of the equilibrium point x .

Theorem 2.2: *Suppose that $r_c \leq 1$.*

- (a) *If $0 < r \leq r_0$, then $\mathcal{B}(0) = [0, c] \cup (x_c, \eta]$ and $\mathcal{B}(1) = (c, x_c)$;*
- (b) *If $r_0 < r \leq \hat{r}$, then $\mathcal{B}(0) = [0, c] \cup (x_c, \eta]$;*
- (c) *If $\hat{r} < r \leq \tilde{r}$, then $\mathcal{B}(0) = [0, \eta] \setminus \Omega$, where Lebesgue measure of Ω is zero, and $\Omega \supset \bigcup_{i=1}^{i=3} \Omega_i$ with*

$$\begin{aligned} \Omega_1 &= \left\{ x \in [c, x_c] \mid f^k(x) = 1, k = 1, 2, \dots \right\}, \\ \Omega_2 &= \left\{ x \in [c, x_c] \mid f^k(x) = c, k = 1, 2, \dots \right\} \end{aligned}$$

and

$$\Omega_3 = \left\{ x \in [c, x_c] \mid f^k(x) = x, k = 2, 3, \dots \right\}$$

are nonempty and countable.

Proof: If $x \in [0, c]$, then $0 \leq f(x) < x$. Hence $\lim_{k \rightarrow \infty} f^k(x) = 0$, i.e. $[0, c] \subset \mathcal{B}(0)$. Furthermore, if $x \in (x_c, \eta]$, then $0 < f(x) < c$. By the previous case, we can also obtain $\lim_{k \rightarrow \infty} f^k(x) = 0$, i.e. $(x_c, \eta] \subset \mathcal{B}(0)$. Thus, $[0, c] \cup (x_c, \eta] \subset \mathcal{B}(0)$.

For (a), we consider the following three cases.



Case 1 $0 < r < \frac{r_0}{2}$. Then $f'(1) > 0$, i.e. $\hat{x} > 1$. If $x \in (c, 1)$, then $f(x) > x > c$ and $f(x) < 1$ and hence $\lim_{k \rightarrow \infty} f^k(x) = 1$. If $x \in (1, \hat{x}]$, then $1 < f(x) < x$ and hence $\lim_{k \rightarrow \infty} f^k(x) = 1$. If $x \in (\hat{x}, x_c)$, then $c = f(x_c) < f(x) < f(\hat{x}) < \hat{x}$, i.e. $f(x) \in (c, \hat{x})$, and hence $\lim_{k \rightarrow \infty} f^k(x) = 1$. In this case, we can obtain that $\mathcal{B}(0) = [0, c) \cup (x_c, \eta]$ and $\mathcal{B}(1) = (c, x_c)$.

Case 2 $r = \frac{r_0}{2}$. Then $\hat{x} = 1$. Using arguments similar to Case 1, we can obtain that the result holds.

Case 3 $\frac{r_0}{2} < r \leq r_0$. Then $-1 \leq f'(1) < 0$, i.e. $\hat{x} < 1$. Since $f(x)$ satisfies (i)-(vi) given in Theorem 2.9 in [2], the equilibrium point 1 is globally asymptotically stable on (c, x_c) if $f(f(x)) > x$ for $x \in [\hat{x}, 1)$ and (c, x_c) is positively invariant for the map f . Let

$$\phi_1(x) = x(1-x)(x-c), \quad \phi_2(x) = -f(x)(1-f(x))(f(x)-c).$$

Then $g(x) = \phi_1(x) - \phi_2(x)$. It follows that

$$\phi'_1(x) = -3x^2 + 2(c+1)x - c, \quad \phi'_2(x) = -f'(x)(-3(f(x))^2 + 2(c+1)f(x) - c).$$

For $x \in [\hat{x}, 1)$, $f(x) \in (1, f(\hat{x})]$. Since $\phi'_1(x)$ is decreasing and $\phi'_2(x)$ is increasing on $[\hat{x}, 1)$, $g'(x)$ has at most a zero point on $[\hat{x}, 1)$. Notice that $g(1) = 0$ and $g'(1) = (c-1)(1+f'(1)) < 0$. Thus $g(x) > 0$ for $x \in [\hat{x}, 1)$. If the result is false then there is a $x_1 \in (\hat{x}, 1)$ for which $g(x_1) \leq 0$. Since $g'(\hat{x}) = -3\hat{x}^2 + 2(c+1)\hat{x} - c < 0$, $g(x)$ have at least two zero points on $[\hat{x}, 1)$. This contradicts $g'(x)$ has at most a zero point on $[\hat{x}, 1)$. This contradiction shows that $f^2(x) > x$ for $x \in [\hat{x}, 1)$. Moreover, $f^2(\hat{x}) > \hat{x} > c = f(x_c)$. The inequality is equivalent to $f(\hat{x}) < x_c$. It follows that (c, x_c) is positively invariant for the map f . Hence, $\mathcal{B}(0) = [0, c) \cup (x_c, \eta]$ and $\mathcal{B}(1) = (c, x_c)$.

(b) If $r_0 < r \leq \tilde{r}$, then $[c, x_c]$ is positively invariant for the map f . Thus, $\mathcal{B}(0) = [0, c) \cup (x_c, \eta]$.

(c) Let $\varrho = \frac{c}{2} + \frac{1}{2}\sqrt{c^2 + \frac{4}{r}}$, then $f(\varrho) = 1$ and $\varrho < x_c$. It easy to obtain that $1, \varrho \in \Omega_1$ and $c, x_c \in \Omega_2$. Let $G_1(x) = \frac{1}{r}(f^2(x) - x)$. Then $G_1(c) = 0$, $G_1(1) = 0$, $G'_1(c) = c(1 - c)(1 + f'(c)) > 0$ and $G'_1(1) = (c-1)(1+f'(1)) > 0$. This shows that $G_1(x)$ have zero points on $(c, 1)$. Thus, Ω_i , $i = 1, 2, 3$ are nonempty and countable. Note that if $\tilde{r} < r \leq \tilde{r}$, then $f^2(\hat{x}) < c$. Based on Theorem 1 in [32], if the map f has a negative Schwartzian derivative, i.e.

$$Sf(x) = \frac{f'''(x)}{f'_2(x)} - \frac{3}{2} \left(\frac{f''(x)}{f'(x)} \right)^2 < 0,$$

then $\lim_{k \rightarrow \infty} f^k(x_0) = 0$ for Lebesgue almost every $x_0 \in [0, \eta]$, i.e. called *essential extinction*. In fact, for $x \geq 0$,

$$Sf(x) = \frac{-12r[2rx^2 + r(2x - (c+1))^2 + 1 - rc]}{2(-3rx^2 + 2r(c+1)x + (1 - rc))^2} < 0.$$

Thus, $\mathcal{B}(0) = [0, \eta] \setminus \Omega$ and $\Omega \supset \bigcup_{i=1}^{i=3} \Omega_i$. □

Remark 1: The equilibrium point 0 is locally asymptotically stable for the model (6), whereas 0 for the classical discrete logistic model is unstable. By the Theorem 2.2, $\mathcal{B}(0) = [0, c) \cup (x_c, \eta]$. It shows that if a population starts with a very little or large initial size, then

due to the Allee effect, the population may not be able to survive. Furthermore, we can find that $\mathcal{B}(1) = (c, x_c)$ becomes small as c increases. From the ecological point of view, with little growth rate, the range of initial size, which makes the population tendency to the steady state, becomes small as the Allee effect constant increases. It is well known that the equilibrium point 1 for the classical discrete logistic model undergoes the flip bifurcation at $r = 2$. However, due to the Allee effect, the flip bifurcation occurs as r increase to r_0 .

3. Stability of the equilibrium points for the predator-prey population

Let

$$\begin{cases} f_1(x, y) = x + rx(1-x)(x-c) - axy, \\ g_1(x, y) = y + ay(x-y), \end{cases}$$

$$\Gamma_1 = \left\{ (x, y) \mid 0 \leq y \leq \frac{1}{a}(1+r(1-x)(x-c)), x \geq 0 \right\}$$

and

$$\Gamma_2 = \left\{ (x, y) \mid 0 \leq y \leq \frac{1}{a} + x, x \geq 0 \right\}.$$

First, assume that $rc \leq 1$, so that $(0, 0) \in \Gamma_1 \cap \Gamma_2$. It is easy to obtain that for $(x, y) \in \Gamma_1 \cap \Gamma_2$, $f_1(x, y) \leq x + rx(1-x)(x-c) \leq f(\hat{x})$ and $g_1(x, y) \leq y + ay(x-y) \leq \frac{(1+a\hat{x})^2}{4a}$. Notice that if $(x, y) \in \Gamma_1 \cap \Gamma_2$, then $f_1(x, y) \geq 0$ and $g_1(x, y) \geq 0$, while if $(x, y) \in (\{(x, y) | x \geq 0, y \geq 0\} \setminus (\Gamma_1 \cap \Gamma_2))$, then $f_1(x, y)$ and $g_1(x, y)$ are at least one less than 0. Thus, considering the ecological meaning, for $(x, y) \in \Gamma_1 \cap \Gamma_2$, if $(f_1(x, y), g_1(x, y)) \notin \Gamma_1 \cap \Gamma_2$ then we take $f_1(x, y) = g_1(x, y) = 0$ which represents larger densities leading to population collapse. Then denote the model (5) as follows

$$\begin{cases} x_{n+1} = f_1(x_n, y_n), \\ y_{n+1} = g_1(x_n, y_n), \end{cases} \quad (x_0, y_0) \in \Gamma_1 \cap \Gamma_2,$$

where (x_0, y_0) are initial conditions. It can obtain that $\Gamma_1 \cap \Gamma_2$ is non-negatively invariant and bounded for the model (5).

Clearly, the model (5) have always the equilibrium points $E_0(0, 0)$, $E_1(c, 0)$ and $E_2(1, 0)$. It easily see that $E_0, E_1, E_2 \in \Gamma_1 \cap \Gamma_2$.

If $r < \frac{a}{(1-\sqrt{c})^2}$, the model (5) has no positive equilibrium point. If $r = \frac{a}{(1-\sqrt{c})^2}$, the model (5) has a unique positive equilibrium point $E_1^*(x_1^*, y_1^*)$, where $x_1^* = y_1^* = \sqrt{c}$. If $r > \frac{a}{(1-\sqrt{c})^2}$, the model (5) have two positive equilibrium points $E_2^*(x_2^*, y_2^*)$ and $E_3^*(x_3^*, y_3^*)$, where

$$x_2^* = y_2^* = \frac{r(c+1)-a-\delta}{2r} \quad \text{and} \quad x_3^* = y_3^* = \frac{r(c+1)-a+\delta}{2r}$$

with

$$\delta = \sqrt{(r(1+\sqrt{c})^2-a)(r(1-\sqrt{c})^2-a)}.$$

It follows from simple computation that $E_i^* \in \text{Int}(\Gamma_1 \cap \Gamma_2)$, $i = 1, 2, 3$ where $\text{Int}(\Gamma_1 \cap \Gamma_2)$ is the interior of $\Gamma_1 \cap \Gamma_2$. First, we study the magnitude of E_3^* with respect to r and c . Differentiating x_3^* with respect to r and c , respectively, and simplifying, we get

$$\frac{dx_3^*}{dr} = \frac{a(r(1+c) - a + \delta)}{2r^2\delta} > 0$$

and

$$\frac{dx_3^*}{dc} = \frac{-2ra}{\delta(r(1-c) + a + \delta)} < 0.$$

When $r = \frac{a}{(1-\sqrt{c})^2}$, the characteristic equation of the equilibrium point $E_1^*(x^*, y^*)$ is $\lambda^2 - 2\lambda + 1 = 0$ and its root is 1 with multiplicity 2. Thus, the equilibrium point $E_1^*(x^*, y^*)$ is non-hyperbolic. For $r > \frac{a}{(1-\sqrt{c})^2}$ there are two positive equilibrium points in the model (5). For $r < \frac{a}{(1-\sqrt{c})^2}$ there are no positive equilibrium points in the model (5). While r crosses $\frac{a}{(1-\sqrt{c})^2}$ from right to left, the two equilibrium points collide, forming at $r = \frac{a}{(1-\sqrt{c})^2}$ an equilibrium point with $\lambda = 1$, and disappear. It can obtain from the Section 4.2 in [21] that the model (5) undergoes fold bifurcation at E_1^* .

Remark 2: One can easily obtain that the model (2) always has a unique positive equilibrium point $E(x^*, y^*)$, where $x^* = y^* = \frac{r}{a+r}$. However, it follows from above discussion that the model (5) may undergo two, one and no positive equilibrium points. In other words, the model (5) occurs fold bifurcation at the existence equilibrium point E_1^* due to the Allee effect. Moreover, the larger positive equilibrium point E_3^* is increasing with respect to the intrinsic growth rate r and decreasing with respect to the Allee constant c .

Next we discuss the stability of the equilibrium points of the model (5). The Jacobian matrix J of the model (5) evaluated at the equilibrium point (x, y) is given by

$$J = \begin{pmatrix} 1 + r(1 - 2x)(x - c) + rx(1 - x) - ay & -ax \\ ay & 1 + a(x - 2y) \end{pmatrix}.$$

The characteristic equation of Jacobian matrix J may be written as

$$H(\lambda) = \lambda^2 - p(x, y)\lambda + q(x, y) = 0$$

where $p(x, y)$ and $q(x, y)$ are the trace and the determinant of J respectively with

$$p(x, y) = 2 + r(1 - 2x)(x - c) + rx(1 - x) - ay + a(x - 2y)$$

and

$$q(x, y) = (1 + r(1 - 2x)(x - c) + rx(1 - x) - ay)(1 + a(x - 2y)) + a^2xy.$$

For the extinction equilibrium point $E_0(0, 0)$, the corresponding characteristic equation is $(\lambda - (1 - rc))(\lambda - 1) = 0$ and its roots are $\lambda_1 = 1 - rc < 1$ and $\lambda_2 = 1$ that means $E_0(0, 0)$ is non-hyperbolic. For the equilibrium point $E_1(c, 0)$, its eigenvalues are $\lambda_1 = 1 + r(1 - c) > 1$ and $\lambda_2 = 1 + ac > 1$. Thus, $E_1(c, 0)$ is unstable. For the equilibrium point $E_2(1, 0)$, its eigenvalues are $\lambda_1 = 1 - r(1 - c)$ and $\lambda_2 = 1 + a > 1$. Thus, $E_2(1, 0)$ is also unstable.

In order to analyze the stability of the equilibrium point $E_0(0, 0)$, we must apply the center manifold theorem [21,37] to study the higher-order terms. Now we rewrite the equations in the model (5) as

$$\begin{cases} x_{n+1} = (1 - rc)x_n + \tilde{f}(x_n, y_n), \\ y_{n+1} = y_n + \tilde{g}(x_n, y_n), \end{cases} \quad (12)$$

where

$$\tilde{f}(x_n, y_n) = r(1 + c)x_n^2 - ax_ny_n - rx_n^3$$

and

$$\tilde{g}(x_n, y_n) = ax_ny_n - ay_n^2.$$

Assume that the center manifold function h takes

$$h(y) = a_2y^2 + a_3y^3 + O(y^4).$$

By using the undetermined coefficient method, we compute the coefficients a_2 and a_3 . The function h must satisfy the center manifold equation

$$h(y + \tilde{g}(h(y), y)) - [(1 - rc)h(y) + \tilde{f}(h(y), y)] = 0.$$

Equating the coefficients of the series, we obtain the system of equations

$$rca_2 = 0$$

and

$$-aa_2 + rca_3 = 0.$$

Solving the above two equations, it follows that $a_2 = a_3 = 0$. Thus on the center manifold $x = h(y)$, we have the following map

$$P(y) = y - ay^2 + O(y^5).$$

Calculations show that $P'(0) = 1$ and $P''(0) = -2a < 0$. By the Theorem 2.3 in [13], the fixed point 0 for the map P is semi-asymptotically stable from the right. Therefore, the extinction equilibrium point $E_0(0, 0)$ for the model (5) is locally asymptotically stable in the region $\{(x, y) | x \geq 0, y \geq 0\}$.

In this following, we discuss the stability of the equilibrium points $E_2^*(x_2^*, y_2^*)$ and $E_3^*(x_3^*, y_3^*)$.

Notice that

$$\begin{aligned} p(x_2^*, y_2^*) &= -2r(x_2^*)^2 + (r(c + 1) - a)x_2^* + 2, \\ q(x_2^*, y_2^*) &= (-2r(x_2^*)^2 + r(c + 1)x_2^* + 1)(1 - ax_2^*) + a^2(x_2^*)^2. \end{aligned}$$

By simple computation, one can obtain

$$H(1)|_{(x,y)=(x_2^*,y_2^*)} = -a(x_2^*)^2\delta < 0.$$

Then $H(\lambda)|_{(x,y)=(x_2^*,y_2^*)} = 0$ has one root lying in $(1, \infty)$. Thus, the equilibrium point E_2^* is unstable.

For the equilibrium point $E_3^*(x_3^*, y_3^*)$, we have

$$p(x_3^*, y_3^*) = 2 - (\alpha_c + a)x_3^*,$$

$$q(x_3^*, y_3^*) = (1 - \alpha_c x_3^*)(1 - ax_3^*) + a^2(x_3^*)^2,$$

where $\alpha_c = r(2x_3^* - (c + 1))$. Let $\tilde{H}(\lambda) = H(\lambda)|_{(x,y)=(x_3^*,y_3^*)}$. Notice that

$$\alpha_c + a = 2rx_3^* - r(c + 1) + a = \delta > 0.$$

Hence,

$$\tilde{H}(1) = a(x_3^*)^2\delta > 0.$$

It follows from the well-known *Jury* conditions (see [30]) that the modulus of all roots of $\tilde{H}(\lambda) = 0$ less than 1 if and only if the conditions

$$\tilde{H}(-1) = a\delta(x_3^*)^2 - 2\delta x_3^* + 4 > 0 \quad (13)$$

and

$$\tilde{H}(0) = a\delta(x_3^*)^2 - \delta x_3^* + 1 < 1 \quad (14)$$

hold. The inequality (14) holds if and only if

$$ax_3^* < 1, \quad \text{i.e. } \frac{a}{r} > \frac{(a-1)(1-ac)}{a}. \quad (15)$$

To discuss the conditions of the inequality (13) holding, we consider the following three cases separately, namely

- (a) $\delta < 4a$, (b) $\delta = 4a$ and (c) $\delta > 4a$.

By simple calculation, one can obtain that

$$\delta < 4a, \quad \text{i.e. } \frac{a}{r} > \frac{(c-1)^2}{(c+1) + \sqrt{(c+1)^2 + 15(c-1)^2}} := c_1.$$

In case (a), it is clear that the inequality (13) holds trivially. In case (b), the inequality (13) holds if

$$ax_3^* \neq 1, \quad \text{i.e. } \frac{a}{r} \neq \frac{(a-1)(1-ac)}{a}.$$

In case (c), the inequality (13) holds if

$$ax_3^* > 1 + k \quad (16)$$

or

$$ax_3^* < 1 - k, \quad (17)$$

where $k = \sqrt{1 - \frac{4a}{\delta}}$ and $0 < k < 1$. Clearly, one can see that the inequality (16) does not hold. In fact, assume the inequality (16) holds. Since $\tilde{H}(1) > 0$ and $\delta > 4a$, $\tilde{H}(\lambda) = 0$ has two roots with $-1 < \lambda_i < 1, i = 1, 2$. Note that $\lambda_1 \lambda_2 = \delta x_3^*(ax_3^* - 1) + 1 > 1$. This is a contradiction. It follows from the inequality (17) that

$$\frac{a}{r} > \frac{(a-1+k)(1-k-ac)}{a(1-k)}. \quad (18)$$

From the above analysis, we can obtain that $\tilde{H}(-1) = 0$ and $\tilde{H}(0) = 1$ hold if and only if $\frac{a}{r} = \frac{(a-1+k)(1-k-ac)}{a(1-k)}$ and $\frac{a}{r} = \frac{(a-1)(1-ac)}{a}$, respectively. Furthermore, one can get the following Theorem 3.1.

Theorem 3.1: *The model (5) have always three equilibrium points $E_0(0, 0)$, $E_1(c, 0)$ and $E_2(1, 0)$, where $E_0(0, 0)$ is local asymptotically stable in the region $\{(x, y) | x \geq 0, y \geq 0\}$ if $rc \leq 1$, and $E_1(c, 0)$ and $E_2(1, 0)$ are unstable. If $r = \frac{a}{(1-\sqrt{c})^2}$, the model (5) has unique positive equilibrium point $E_1^*(x_1^*, y_1^*)$, where $E_1^*(x_1^*, y_1^*)$ is unstable. If $r > \frac{a}{(1-\sqrt{c})^2}$, the model (5) have two positive equilibrium points $E_2^*(x_2^*, y_2^*)$ and $E_3^*(x_3^*, y_3^*)$, where $E_2^*(x_2^*, y_2^*)$ is unstable. Furthermore, $E_3^*(x_3^*, y_3^*)$ is a stable focus if $\frac{a}{r} > \max\left\{c_1, \frac{(a-1)(1-ac)}{a}\right\}$, a stable critical node if $\frac{a}{r} = c_1 > \frac{(a-1)(1-ac)}{a}$, a stable node if $\frac{(a-1+k)(1-k-ac)}{a(1-k)} < \frac{a}{r} < c_1$, a saddle if $\frac{(a-1-k)(1+k-ac)}{a(1-k)} < \frac{a}{r} < \min\left\{c_1, \frac{(a-1)(1-ac)}{a}\right\}$, a unstable focus if $c_1 < \frac{a}{r} < \frac{(a-1)(1-ac)}{a}$.*

Remark 3: The extinction equilibrium point $(0, 0)$ for the model (2) is always unstable and the unique existence equilibrium point may be asymptotically stable. However, Theorem 3.1 implies that both the extinction equilibrium point and the existence equilibrium point may be stable for the model (5). It shows that the model (5) possesses a dynamical bistability phenomenon due to Allee effects.

In the following, we consider the case that the positive equilibrium point $E_3^*(x_3^*, y_3^*)$ is non-hyperbolic. Then always assume $r > \frac{a}{(1-\sqrt{c})^2}$. By the relation between roots and coefficients, $\tilde{H}(\lambda) = 0$ have a simple root -1 if and only if $\tilde{H}(-1) = 0$ and $\tilde{H}'(-1) \neq 0$, a pair of conjugate complex roots if and only if $p(x_3^*, y_3^*)^2 - 4q(x_3^*, y_3^*) < 0$ and $\tilde{H}(0) = 1$. Let

$$M_1 = \left\{ (r, c, a) \left| \frac{(a-1+k)(1-k-ac)}{a(1-k)} = \frac{a}{r} < c_1 \right. \right\},$$

$$M_2 = \left\{ (r, c, a) \left| c_1 < \frac{a}{r} = \frac{(a-1)(1-ac)}{a} \right. \right\}.$$

From the inequality (15) and (17), if $(r, c, a) \in M_1$, then the eigenvalues of the equilibrium point $E_3^*(x_3^*, y_3^*)$ are $\lambda_1 = -1$ and $|\lambda_2| < 1$. Thus, the model (5) may undergo the flip bifurcation at the equilibrium point $E_3^*(x_3^*, y_3^*)$. Similarly, if $(r, c, a) \in M_2$, then the eigenvalues of the equilibrium point $E_3^*(x_3^*, y_3^*)$ are a pair of conjugate complex roots with modulus 1. In this case, the model (5) may undergo the Neimark–Sacker bifurcation at the equilibrium point $E_3^*(x_3^*, y_3^*)$.

4. Codimension-one bifurcations for the positive equilibrium point E_3^*

In this section, we discuss the flip bifurcation and the Neimark–Sacker bifurcation at the equilibrium point $E_3^*(x_3^*, y_3^*)$. Let $u_n = x_n - x_3^*$, $v_n = y_n - y_3^*$. We can transform the equilibrium point $E_3^*(x_3^*, y_3^*)$ into the origin

$$\begin{aligned} u_{n+1} &= u_n + r(u_n + x_3^*)(1 - u_n - x_3^*)(u_n + x_3^* - c) - a(u_n + x_3^*)(v_n + y_3^*), \\ v_{n+1} &= v_n + a(v_n + y_3^*)(u_n + x_3^* - v_n - y_3^*). \end{aligned} \quad (19)$$

Introducing a new variable $X_n = (u_n, v_n)^T$, we can rewrite (19) in the form

$$X_{n+1} = \tilde{F}(X_n) = AX_n + \frac{1}{2}B(X_n, X_n) + \frac{1}{6}C(X_n, X_n, X_n) + O(\|X_n\|^4), \quad (20)$$

where

$$A = \begin{pmatrix} 1 - \alpha_c x_3^* & -ax_3^* \\ ax_3^* & 1 - ax_3^* \end{pmatrix},$$

$B(X_n, X_n)$ and $C(X_n, X_n, X_n)$ are multi-linear functions with

$$B(X_n, X_n) = (\beta u_n^2 - 2au_nv_n, 2au_nv_n - 2av_n^2)^T,$$

$$C(X_n, X_n, X_n) = (-6ru_n^3, 0)^T$$

and $\beta = 3a - r(c + 1) - 3\delta$.

4.1. Flip bifurcation

Next we choose r as the bifurcation parameter. Assume that $(r, a, c) \in M_1$. Denote the critical value $r = \frac{a^2(1-k)}{(a-1+k)(1-k-ac)}$ by r_1 at which the map (20) may undergo the flip bifurcation at the origin. Let $r = r_1$. In this case, A has a simple critical eigenvalue $\lambda_1 = -1$, and the corresponding critical eigenspace T^C is one-dimensional and spanned by an eigenvector $\tilde{q} \in \mathbb{R}^2$ such that $A\tilde{q} = -\tilde{q}$. Let $\tilde{p} \in \mathbb{R}^2$ be the adjoint eigenvector, i.e. $A^T\tilde{p} = -\tilde{p}$, where A^T is the transposed matrix of A . Normalize \tilde{p} with respect to \tilde{q} such that $\langle \tilde{p}, \tilde{q} \rangle = 1$, where $\langle \tilde{p}, \tilde{q} \rangle$ is the scalar product in \mathbb{R}^2 . For satisfying the normalization $\langle \tilde{p}, \tilde{q} \rangle = 1$, we can choose

$$\tilde{q} = (\tilde{q}_{01}, \tilde{q}_{02})^T = (-1 - k, 1 - k)^T, \tilde{p} = (\tilde{p}_{01}, \tilde{p}_{02})^T = \frac{1}{4k}(-1 - k, k - 1)^T.$$

Based on the theories developed by Kuznetsov [21], the restriction of the map (20) to its one dimensional center manifold at the critical parameter values r_1 can be transformed into the normal form

$$\xi \mapsto -\xi + d\xi^3 + O(\xi^4),$$

where

$$\begin{aligned} d &= \frac{1}{6}\langle \tilde{p}, C(\tilde{q}, \tilde{q}, \tilde{q}) \rangle - \frac{1}{2}\langle \tilde{p}, B(\tilde{q}, (A - I)^{-1}B(\tilde{q}, \tilde{q})) \rangle \\ &= -r\tilde{p}_{01}\tilde{q}_{01}^3 - \frac{r}{\delta(r(c + 1) - a + \delta)}[\tilde{p}_{01}(\beta(a - \beta)\tilde{q}_{01}^3 \\ &\quad + (5\beta - 4a + 2\delta)a\tilde{q}_{01}^2\tilde{q}_{02} - 2(\beta + \delta + a)a\tilde{q}_{01}\tilde{q}_{02}^2 + 2a^2\tilde{q}_{02}^3) \\ &\quad + \tilde{p}_{02}(a\beta\tilde{q}_{01}^3 + a(3\beta + 2\delta - 4a)\tilde{q}_{01}^2\tilde{q}_{02} + 2a(\delta - 5a)\tilde{q}_{01}\tilde{q}_{02}^2 + 2a(3a - 2\delta)\tilde{q}_{02}^3)] \\ &= -\frac{r(1+k)^4}{4k} - \frac{r}{4k\delta(r(c + 1) - a + \delta)}[(4a^2 - \beta^2)k^4 - 4(2a^2 - 3a\beta + 2a\delta + \beta^2)k^3 \\ &\quad - 2(20a^2 - 16a\delta - 8a\beta + 3\beta^2)k^2 - 4(\beta^2 - 14a^2 + 6a\delta + a\beta)k \\ &\quad - (\beta^2 + 8a\beta + 12a^2)] \end{aligned}$$

and I is the unit 2×2 matrix.

Notice that $\delta > 4a$ and $\beta = 3a - r(c + 1) - 3\delta$. We can obtain that

$$\begin{aligned} \frac{\beta^2 - 4a^2}{\delta(r(c+1) - a + \delta)} &= \frac{(\beta - 2a)(\beta + 2a)}{\delta(r(c+1) - a + \delta)} > 1, \\ \frac{2a^2 - 3a\beta + 2a\delta + \beta^2}{\delta(r(c+1) - a + \delta)} &> 1, \\ \frac{20a^2 - 16a\delta - 8a\beta + 3\beta^2}{\delta(r(c+1) - a + \delta)} &= \frac{20a^2 - 8a(2\delta + \beta) + 3\beta^2}{\delta(r(c+1) - a + \delta)} > 3, \\ \frac{\beta^2 - 14a^2 + 6a\delta + a\beta}{\delta(r(c+1) - a + \delta)} &= \frac{\beta(\beta + a) + 2a(-7a + 3\delta)}{\delta(r(c+1) - a + \delta)} > 1, \\ \frac{\beta^2 + 8a\beta + 12a^2}{\delta(r(c+1) - a + \delta)} &= \frac{(\beta + 2a)(\beta + 6a)}{\delta(r(c+1) - a + \delta)} > 1. \end{aligned}$$

It follows that $d > 0$. Thus, we can obtain the following theorem.

Theorem 4.1: If $r > \frac{a}{(1-\sqrt{c})^2}$ and $(r, c, a) \in M_1$, then the model (5) undergoes the flip bifurcation at the equilibrium point $E_3^*(x_3^*, y_3^*)$ when the parameter r varies and passes through r_1 . Moreover, by $d > 0$, the flip bifurcation of the model (5) at $r = r_1$ is supercritical and the period-doubling cycle is stable.

4.2. Neimark-Sacker bifurcation

Next we choose also r as the bifurcation parameter. Assume that $(r, a, c) \in M_2$. Denote the critical value $r = \frac{a^2}{(a-1)(1-ac)}$ by r_2 at which the map (20) may undergo the Neimark-Sacker bifurcation at the origin. In this case, A has a simple pair of complex eigenvalues on the unit circle: $\lambda_{1,2} = e^{\pm i\theta_0}$, where

$$\theta_0 = \arccos \frac{1 - \alpha_c x_3^*}{2}.$$

Let $\hat{q} \in \mathbb{C}^2$ be a complex eigenvector corresponding to λ_1 :

$$A\hat{q} = e^{i\theta_0}\hat{q}.$$

The critical real eigenspace T^C corresponding to $\lambda_{1,2}$ is two-dimensional and is spanned by $\{\operatorname{Re}\hat{q}, \operatorname{Im}\hat{q}\}$.

Introduce also the adjoint eigenvector $\hat{p} \in \mathbb{C}^2$ having the properties

$$A^T \hat{p} = e^{-i\theta_0} \hat{p}.$$

Normalize also \hat{p} with respect to \hat{q} such that $\langle \hat{p}, \hat{q} \rangle = 1$, where $\langle \hat{p}, \hat{q} \rangle$ is the scalar product in \mathbb{C}^2 . For satisfying the normalization $\langle \hat{p}, \hat{q} \rangle = 1$, we can choose

$$\hat{q} = (1, e^{-i\theta_0})^T, \quad \hat{p} = \frac{1}{1 - e^{2i\theta_0}} (1, -e^{i\theta_0})^T.$$

Notice that $|\lambda_{1,2}| = \sqrt{q(x_3^*, y_3^*)}$. Since

$$\frac{dx_3^*}{dr} = \frac{a(r(1+c) - a + \delta)}{2r^2\delta} > 0,$$

we can obtain that

$$l = \left. \frac{d |\lambda_{1,2}|^2}{dr} \right|_{r=r_2} = \left[\delta \frac{dx_3^*}{dr} \right]_{r=r_2} > 0.$$

Therefore, the transversality condition is satisfied. Moreover, it is required that when $r = r_2$, $\lambda_{1,2}^m \neq 1, m = 1, 2, 3, 4$ (no strong resonances), which is equivalent to $p(x_3^*, y_3^*)|_{r=r_2} \neq -2, -1, 0, 2$. Note $(r_2, c, a) \in M_2$, then $p(x_3^*, y_3^*)|_{r=r_2} \neq \pm 2$. Therefore, we only need to require that $p(x_3^*, y_3^*)|_{r=r_2} \neq 0, -1$, which leads to

$$\nu = \left. \frac{\delta(r(c+1) - a + \delta)}{r} \right|_{r=r_2} \neq 4, 6. \quad (21)$$

Hence, if the inequality (21) holds, then the first non-degeneracy condition for the Neimark–Sacker bifurcation is satisfied.

Based on the theories developed by Kuznetsov [21], the restriction of the map (20) to its two dimensional center manifold at the critical parameter value r_2 can be transformed into the normal form

$$z \mapsto e^{i\theta_0} z(1 + b|z|^2) + O(|z|^4),$$

where

$$\begin{aligned} b &= \frac{1}{2} e^{-i\theta_0} [\langle \hat{p}, C(\hat{q}, \hat{q}, \bar{\hat{q}}) \rangle + 2\langle \hat{p}, B(\hat{q}, (I-A)^{-1}B(\hat{q}, \bar{\hat{q}})) \rangle \\ &\quad + \langle \hat{p}, B(\bar{\hat{q}}, (e^{2i\theta_0} I - A)^{-1}B(\hat{q}, \bar{\hat{q}})) \rangle] \\ &= \frac{1}{2} e^{-i\theta_0} [-\frac{6r}{1 - e^{2i\theta_0}} + \frac{2}{(1 + \alpha_c x_3^*)(1 - e^{2i\theta_0})} (2a^2 \alpha_c x_3^* e^{3i\theta_0} + (a + 2\beta - 5a\alpha_c x_3^*)ae^{2i\theta_0} \\ &\quad + (3a\alpha_c x_3^* - 4\beta - a)ae^{i\theta_0} + (\beta^2 + a\beta + 3a^2 + a^2 \alpha_c x_3^*) + (a - 2\beta - a\alpha_c x_3^*)ae^{-i\theta_0}) \\ &\quad + \frac{1}{e^{-2i\theta_0}(e^{-2i\theta_0} + \alpha_c x_3^* - 1) + 1} (2a^2(\alpha_c x_3^* - 1)e^{3i\theta_0} + 2(\beta - 2a(\alpha_c x_3^* - 1))ae^{2i\theta_0} \\ &\quad + (2a(\alpha_c x_3^* - 1) - 3\beta)ae^{i\theta_0} + (\beta - 2a)a + 2(2a - \beta)ae^{-i\theta_0} \\ &\quad + (\beta^2 + 2a^2 - a\beta)e^{-2i\theta_0} - a\beta e^{-3i\theta_0})]. \end{aligned}$$

Theorem 4.2: Assume $r > \frac{a}{(1-\sqrt{c})^2}$ and $(r, c, a) \in M_2$. If the inequality (21) holds and $\text{Re}b \neq 0$, then the model (5) undergoes the Neimark–Sacker bifurcation at the equilibrium point $E_3^*(x_3^*, y_3^*)$ when the parameter r varies and passes through r_2 . Moreover, since $l > 0$, if $\text{Re}b < 0$ (respectively, $\text{Re}b > 0$), the bifurcation is supercritical (respectively, subcritical) and the closed invariant curve bifurcating from the equilibrium point $E_3^*(x_3^*, y_3^*)$ is stable (respectively, unstable).

It is not easy to determine the value of b analytically. We use numerical examples to illustrate that it is possible for the model (5) to exhibit a supercritical or subcritical Neimark–Sacker bifurcation (see Table 2).

Table 2. The bifurcation direction of Neimark-Sacker bifurcations.

c	a	r_2	$a - r_2 c_1$	ν	Reb	Bifurcation direction
0.1	1.25	7.1429	0.0333	7.7143	-59.4714	Supercritical
0.1	1.30	6.4751	0.1970	6.3678	-163.37	Supercritical
0.1	1.35	6.0198	0.3246	5.4021	64.546	Subcritical
0.3	1.30	9.2350	0.2493	5.3880	93.742	Subcritical

Remark 4: From the population ecological point of view, a closed stable invariant curve bifurcates from the equilibrium point as the growth rate r passes through the critical value, which means that prey and predator can coexist in a stable way and reproduce their densities. Moreover, we can find that when the predator parameter a with $1 < a < \frac{1}{c}$, the bifurcation critical value r_2 increases as the Allee constant c increases.

5. Resonance 1:2 for the equilibrium point E_3^*

By the relation between roots and coefficients, $\tilde{H}(\lambda) = 0$ has a root -1 with multiplicity 2 if and only if $\tilde{H}(-1) = 0$ and $\tilde{H}'(0) = 1$. Let

$$M_3 = \left\{ (r, c, a) \mid c_1 = \frac{a}{r} = \frac{(a-1)(1-ac)}{a} < (1-\sqrt{c})^2 \right\}.$$

It is clear that if $(r, c, a) \in M_3$, then the two eigenvalues of the equilibrium point $E_3^*(x_3^*, y_3^*)$ equal to -1 . Thus, the model (5) may undergo codimension-two bifurcation with 1:2 resonance at $E_3^*(x_3^*, y_3^*)$. In this case,

$$A = \tilde{A} = \begin{pmatrix} -2 & -1 \\ 1 & 0 \end{pmatrix}$$

has an eigenvalue -1 with multiplicity 2.

By the Section 4.5 in [22], we take the truncated normal form for this bifurcation as follows

$$\begin{pmatrix} w_1 \\ w_2 \end{pmatrix} \mapsto \tilde{G}(w) = \begin{pmatrix} -w_1 + w_2 \\ -w_2 + \frac{1}{6}\tilde{c}w_1^3 + \frac{1}{2}\tilde{d}w_1^2w_2 \end{pmatrix}. \quad (22)$$

Next we introduce eigenvectors of \tilde{A} such that

$$\tilde{A}\tilde{q}_0 = -\tilde{q}_0, \quad \tilde{A}\tilde{q}_1 = -\tilde{q}_1 + \tilde{q}_0$$

and similarly for the transposed matrix \tilde{A}^T

$$\tilde{A}^T\tilde{p}_1 = -\tilde{p}_1, \quad \tilde{A}^T\tilde{p}_0 = -\tilde{p}_0 + \tilde{p}_1.$$

For satisfying

$$\langle \tilde{p}_0, \tilde{q}_0 \rangle = \langle \tilde{p}_1, \tilde{q}_1 \rangle = 1, \quad \langle \tilde{p}_0, \tilde{q}_1 \rangle = \langle \tilde{p}_1, \tilde{q}_0 \rangle = 0,$$

we can choose

$$\tilde{q}_0 = (1, -1)^T, \quad \tilde{q}_1 = (0, -1)^T, \quad \tilde{p}_0 = (1, 0)^T, \quad \tilde{p}_1 = (-1, -1)^T.$$

Take the center manifold function $\tilde{H}(w_1, w_2)$ the form as follows

$$\tilde{H}(w_1, w_2) = w_1 \tilde{q}_0 + w_2 \tilde{q}_1 + \sum_{2 \leq j+k \leq 3} \frac{1}{j!k!} \tilde{h}_{jk} w_1^j w_2^k + O(\|w\|^4), \quad (23)$$

where $\tilde{h}_{jk} \in \mathbb{R}^2$. Substituting (23) into (20) and (22) into (23), we have

$$\tilde{F}(\tilde{H}(w)) = \tilde{A}\tilde{H}(w) + \frac{1}{2}B(\tilde{H}(w), \tilde{H}(w)) + \frac{1}{6}C(\tilde{H}(w), \tilde{H}(w), \tilde{H}(w)) + O(\|\tilde{H}(w)\|^4)$$

and

$$\begin{aligned} \tilde{H}(\tilde{G}(w)) &= (-w_1 + w_2)\tilde{q}_0 + \left(-w_2 + \frac{1}{6}\tilde{c}w_1^3 + \frac{1}{2}\tilde{d}w_1^2 w_2 \right) \tilde{q}_1 \\ &\quad + \sum_{2 \leq j+k \leq 3} \frac{1}{j!k!} \tilde{h}_{jk} (-w_1 + w_2)^j \left(-w_2 + \frac{1}{6}\tilde{c}w_1^3 + \frac{1}{2}\tilde{d}w_1^2 w_2 \right)^k + O(\|\tilde{G}(w)\|^4). \end{aligned}$$

Similarly we obtain the following *homological equaiton* for \tilde{H}

$$\tilde{H}(\tilde{G}(w)) = \tilde{F}(\tilde{H}(w)).$$

Comparing the quadratic terms, we obtain

$$\tilde{h}_{20} = -\frac{1}{2}(\gamma - 3a, \gamma + 5a)^T, \tilde{h}_{11} = \left(2a, -\frac{\gamma}{2} - \frac{7}{2}a \right)^T, \tilde{h}_{02} = \frac{1}{4}(\gamma + 9a, -\gamma - 17a)^T,$$

where $\gamma = 3rx_3^* - r(c+1)$. From the cubic terms we can obtain

$$\tilde{c} = \langle \tilde{p}_1, C(\tilde{q}_0, \tilde{q}_0, \tilde{q}_0) \rangle + 3\langle \tilde{p}_1, B(\tilde{q}_0, \tilde{h}_{20}) \rangle = 15a^2 + 12a\gamma - 3\gamma^2 + 6r.$$

Notice that $\frac{a}{r} = \frac{(a-1)(1-ac)}{a}$. By calculations, we can see that one nondegeneracy condition

$$\begin{aligned} \tilde{c} &= r \left(-\frac{3}{4} \left(c + 1 - \frac{a}{r} \right) (11a + r(c+1)) + 6 \right) \\ &= r \left(-\frac{3(1+a^2c)}{4a} (11a + r(c+1)) + 6 \right) < 0 \end{aligned}$$

holds. Since

$$\langle \tilde{p}_0, (\tilde{A} + I)\tilde{h}_{30} \rangle = \langle \tilde{p}_0, \tilde{A}\tilde{h}_{30} \rangle + \langle \tilde{p}_0, \tilde{h}_{30} \rangle = \langle \tilde{A}^T \tilde{p}_0, \tilde{h}_{30} \rangle + \langle \tilde{p}_0, \tilde{h}_{30} \rangle = \langle \tilde{p}_1, \tilde{h}_{30} \rangle,$$

from the equation at the $w_1^2 w_2$ term, we can have

$$\begin{aligned} \tilde{d} &= \langle \tilde{p}_1, 2B(\tilde{q}_0, \tilde{h}_{11}) + \langle \tilde{p}_1, B(\tilde{q}_1, \tilde{h}_{20}) \rangle + \langle \tilde{p}_1, C(\tilde{q}_0, \tilde{q}_0, \tilde{q}_1) \rangle \\ &\quad + \langle \tilde{p}_0, 3B(\tilde{q}_0, \tilde{h}_{20}) + C(\tilde{q}_0, \tilde{q}_0, \tilde{q}_0) \rangle \\ &= 31a^2 + 2a\gamma + 3\gamma^2 - 6r. \end{aligned}$$

Notice that another nondegeneracy condition

$$\tilde{c} + \tilde{d} = 32a^2 + 7a(r(c+1) - a + 3\delta) > 0$$

holds.

Applying the above discussion, we obtain the following results.

Theorem 5.1: Assume that $(r, a, c) \in M_3$. Then the model (5) undergoes a bifurcation with resonance 1:2 at the equilibrium point $E_3^*(x_3^*, y_3^*)$. By $\tilde{c} < 0$, there is a Neimark–Sacker curve of cycles of the model (5) with double period that emanates from the flip bifurcation curve $r = \frac{a^2(1-k)}{(a-1+k)(1-k-ac)}$ of the equilibrium point $E_3^*(x_3^*, y_3^*)$.

6. Marotto's Chaos

In this section, we will discuss the chaotic behaviour for the model (5) in the sense of Marotto [27,28]. In order to analyze the chaotic behaviour for the model (5), we first give the condition under which the equilibrium point $E_3^*(x_3^*, y_3^*)$ is a snap-back repeller. $\hat{H}(\lambda)$ has a pair of conjugate complex roots λ_1 and λ_2 , and $|\lambda_1| = |\lambda_2| > 1$ if and only if

$$p(x, y)^2 - 4q(x, y) < 0, q(x, y) - 1 > 0.$$

Let $w_1(x, y) = p(x, y)^2 - 4q(x, y)$ and $S_1 = \{(x, y) | w_1(x, y) < 0, x > 0, y > 0\}$. By simple computation, it follows that

$$w_1(x, y) = a^2y^2 + (2\alpha_1 - 4ax)ay + \alpha_1^2,$$

where

$$\alpha_1 = r(1 - 2x)(x - c) + rx(1 - x) - ax.$$

If $\Delta_1 = (2a\alpha_1 - 4a^2x)^2 - 4\alpha_1^2a^2 = 16a^3x(ax - \alpha_1) > 0$, the equation $w_1(x, y) = 0$ has two real roots

$$v_1 = \frac{2ax - \alpha_1 - 2\sqrt{ax(ax - \alpha_1)}}{a}, \quad v_2 = \frac{2ax - \alpha_1 + 2\sqrt{ax(ax - \alpha_1)}}{a}$$

and $0 < v_1 < v_2$.

Meanwhile, $\Delta_1 > 0$ is equivalent to $3rx^2 + 2(a - r(c+1))x + rc > 0$. Since

$$(r(c+1) - a)^2 - 3r^2c > (r(1 + \sqrt{c})^2 - a)(r(1 - \sqrt{c})^2 - a) > 0,$$

from $\Delta_1 > 0$ we obtain that $x < u_1$ and $x > u_2$ where

$$u_1 = \frac{(r(c+1) - a) - \sqrt{(r(c+1) - a)^2 - 3r^2c}}{3r},$$

$$u_2 = \frac{(r(c+1) - a) + \sqrt{(r(c+1) - a)^2 - 3r^2c}}{3r}.$$

Thus $S_1 = \{(x, y) | x \in (0, u_1) \cup (u_2, \infty), y \in (v_1, v_2)\}$.



On the other hand, let $w_2(x, y) = q(x, y) - 1$ and $S_2 = \{(x, y) | w_2(x, y) > 0, x > 0, y > 0\}$. By simple computation, it follows that

$$w_2(x, y) = 2a^2y^2 - a(1 + 2\alpha_2)y + \alpha_2(1 + ax) - 1,$$

where $\alpha_2 = 1 + r(1 - 2x)(x - c) + rx(1 - x)$.

If $\Delta_2 < 0$, then $w_2(x, y) > 0$ always holds, where $\Delta_2 = a^2(1+2\alpha_2)^2 - 8a^2(\alpha_2(1+ax)-1)$. If $\Delta_2 \geq 0$, then $w_2(x, y) = 0$ has one real roots with multiplicity 2 or two real roots

$$\nu_3 = \frac{a(1 + 2\alpha_2) - \sqrt{\Delta_2}}{4a^2}, \quad \nu_4 = \frac{a(1 + 2\alpha_2) + \sqrt{\Delta_2}}{4a^2}.$$

Furthermore, if $\alpha_2(1 + ax) - 1 > 0$ and $1 + 2\alpha_2 > 0$, then $0 < \nu_3 \leq \nu_4$; If $\alpha_2(1 + ax) - 1 > 0$ and $1 + 2\alpha_2 < 0$, then $\nu_3 \leq \nu_4 < 0$; If $\alpha_2(1 + ax) - 1 < 0$, then $\nu_3 < 0 < \nu_4$. Notice that

$$\alpha_2(1 + ax) - 1 = -3arx^3 + r(2a(c + 1) - 3)x^2 + (2r(c + 1) + (1 - rc)a)x - rc =: h_1(x).$$

Since $2r(c + 1) + (1 - rc)a > 0$, $h_1(x)$ has unique zero point u_3 on $(0, \infty)$. And $h_1(x) > 0 (< 0)$ for $x < u_3 (> u_3)$. Let

$$1 + 2\alpha_2 = -6rx^2 + 4r(c + 1)x + 3 - 2rc =: h_2(x).$$

Then $h_2(x)$ has unique zero point

$$u_4 = \frac{2r(c + 1) + \sqrt{(2r(c + 1))^2 + 6r(3 - 2rc)}}{6r}$$

on $(0, \infty)$. And $h_2(x) > 0 (< 0)$ for $x < u_4 (> u_4)$. Denote $u_5 = \min\{u_3, u_4\}$. By $\Delta_2 \geq 0$, we can obtain

$$\begin{aligned} (2\alpha_2 - 1)^2 - 8(ax\alpha_2 - 1) &= (-6rx^2 + 4r(c + 1)x + 1 - 2rc)^2 \\ &\quad - 8ax(-3rx^2 + 2r(c + 1)x + 1 - rc) + 8 \geq 0. \end{aligned}$$

Let $D_1 = \{x | \alpha_3 \geq 0\}$ and $D_2 = \{x | \alpha_3 < 0\}$, where

$$\alpha_3 = (-6rx^2 + 4r(c + 1)x + 1 - 2rc)^2 - 8ax(-3rx^2 + 2r(c + 1)x + 1 - rc) + 8.$$

Denote $S_{21} = \{(x, y) | x \in D_1 \cup (0, u_5), y \in (0, \nu_3) \cup (\nu_4, \infty)\}$, $S_{22} = \{(x, y) | x \in D_1 \cup (u_3, \infty), y \in (\nu_4, \infty)\}$ and $S_{23} = \{(x, y) | x \in D_2, y \in (0, \infty)\}$, respectively. Thus $S_2 = S_{21} \cup S_{22} \cup S_{23}$.

According to the above analysis, we obtain the following lemma.

Lemma 6.1: *Let $r > \frac{a}{(1-\sqrt{c})^2}$. If $(x, y) \in S_1 \cap S_2$, then $p(x, y)^2 - 4q(x, y) < 0$, $q(x, y) - 1 > 0$ and $x > 0, y > 0$. Moreover, if the fixed point $E_3^*(x_3^*, y_3^*)$ for the model (5) satisfies $E_3^*(x_3^*, y_3^*) \in S_1 \cap S_2$, then $E_3^*(x_3^*, y_3^*)$ is an expanding fixed point in $S_1 \cap S_2$.*

By the definition of a snap-back repeller [27], we must find one point $(x_1, y_1) \in S_1 \cap S_2$ such that $(x_1, y_1) \neq (x_3^*, y_3^*)$, $F^M(x_1, y_1) = (x_3^*, y_3^*)^T$ and $|DF^k(x_1, y_1)| \neq 0$ for some positive integer M and $1 \leq k \leq M$, where F is defined by the map (5) for the model (5) and F^k is the k times iterations.

Notice that

$$\begin{cases} x_1 + rx_1(1 - x_1)(x_1 - c) - ax_1y_1 = x_2, \\ y_1 + ay_1(x_1 - y_1) = y_2. \end{cases} \quad (24)$$

and

$$\begin{cases} x_2 + rx_2(1 - x_2)(x_2 - c) - ax_2y_2 = x_3^*, \\ y_2 + ay_2(x_2 - y_2) = y_3^*. \end{cases} \quad (25)$$

In the following, if there are solutions different from (x_3^*, y_3^*) for Equations (24) and (25), then a map F^2 has been constructed to map (x_1, y_1) to (x_3^*, y_3^*) . From the Equations (25), we can obtain that the solutions (x_2, y_2) satisfy the following equations

$$\begin{cases} [x_2 + rx_2(1 - x_2)(x_2 - c) - x_3^*][ax_2^2 - rx_2(1 - x_2)(x_2 - c) + x_3^*] - ay_3^*x_2^2 = 0, \\ y_2 = \frac{1}{ax_2}(x_2 + rx_2(1 - x_2)(x_2 - c) - x_3^*). \end{cases} \quad (26)$$

Substituting x_2 and y_2 into Equations (24) and solving x_1, y_1 , one have

$$\begin{cases} [x_1 + rx_1(1 - x_1)(x_1 - c) - x_2][ax_1^2 - rx_1(1 - x_1)(x_1 - c) + x_2] - ay_2x_1^2 = 0, \\ y_1 = \frac{1}{ax_1}(x_1 + rx_1(1 - x_1)(x_1 - c) - x_2). \end{cases} \quad (27)$$

Since $(x_1, y_1) \in S_1 \cap S_2$, $|DF(x_1, y_1)| > 1 \neq 0$. For $|DF^2(x_1, y_1)|$, we can obtain

$$|DF^2(x_1, y_1)| = (d_1d_2 - ae_2d_2 - a^2e_1y_1)(d_3(1 + ax_1 - 2ay_1) - a^2e_2x_1) - a^2[x_1(ae_2 - d_1) - e_1(1 + ax_1 - 2ay_1)](d_3y_1 + e_2d_2),$$

where

$$\begin{aligned} e_1 &= x_1 + rx_1(1 - x_1)(x_1 - c) - ax_1y_1, \\ e_2 &= y_1 + ay_1(x_1 - y_1), \\ d_1 &= -3re_1^2 + 2r(c + 1)e_1 + 1 - rc, \\ d_2 &= -3rx_1^2 + 2r(c + 1)x_1 + 1 - rc - ay_1, \\ d_3 &= 1 - 2ae_2 + ae_1. \end{aligned}$$

Furthermore, $p(x_3^*, y_3^*)^2 - 4q(x_3^*, y_3^*) < 0$ and $q(x_3^*, y_3^*) > 1$ are equivalent to $\delta < 4a$, i.e. $\frac{a}{r} > c_1$ and $\frac{a}{r} < \frac{(a-1)(1-ac)}{a}$, respectively.

According to the above analysis, the following theorem holds.

Theorem 6.2: Let $r > \frac{a}{(1-\sqrt{c})^2}$. If

$$(H_1) c_1 < \frac{a}{r} < \frac{(a-1)(1-ac)}{a};$$

(H₂) the solutions (x_2, y_2) and (x_1, y_1) of Equations (24) and (25) satisfy $(x_i, y_i) \neq (x_3^*, y_3^*)$, $i = 1, 2$, $(x_1, y_1) \in S_1 \cap S_2$ and $|DF^2(x_1, y_1)| \neq 0$, then (x_3^*, y_3^*) is a snap-back repeller of the map F . Moreover, the map F is chaotic in the sense of Marotto.

Next, for illustrating the existence of conditions in Theorem 6.2, we choose specific parameters values (see Table 3).

**Table 3.** Values of the parameters for chaotic in the sense of Marotto

r	c	a	(x_3^*, y_3^*)	(x_1, y_1)	$w_1(x_1, y_1)$	$w_2(x_1, y_1)$	$ DF^2(x_1, y_1) $
4	0.01	2.5	(0.485, 0.485)	(0.612, 1.003)	-13.401	1.641	-0.574
4	0.01	3	(0.360, 0.360)	(0.552, 0.846)	-14.102	0.702	8.261
4	0.02	2.5	(0.536, 0.536)	(0.787, 0.627)	-13.183	1.505	-1.412
4.5	0.01	2.5	(0.554, 0.554)	(0.641, 1.023)	-14.975	2.609	1.957

Table 3 shows that the parameter values satisfy the conditions of Lemma 6.1 and Theorem 6.2. In fact, we can see $(x_3^*, y_3^*), (x_1, y_1) \in S_1 \cap S_2$, $F^2(x_1, y_1) = (x_3^*, y_3^*)^T$ and $|DF^2(x_1, y_1)| \neq 0$. Thus, each (x_3^*, y_3^*) in the Table 3 is a snap-back repeller.

7. Numerical simulations

In this section, we will give some numerical simulations, including bifurcation diagrams, sensitivity dependence on the initial values, Lyapunov exponents, time sequence diagram and phase portraits, to illustrate the above analytic results and to show the more complex dynamical behaviour of the model (5) with the parameters varying.

Sensitivity to initial values means that each point in such a map is arbitrarily closely approximated by other points with significantly different future trajectories. Thus, an arbitrarily small perturbation of the current trajectory may lead to significantly different future behaviour. Lyapunov exponent of a map is a quantity that characterized the rate of separation infinitesimally close trajectories [31]. Negative, zero and positive Lyapunov exponent indicates that the map exhibits asymptotic stability, some sort of steady state mode and chaotic nature respectively.

7.1. Numerical simulations on stability, flip bifurcation and chaos of the equilibrium point 1 for the prey

Time sequence diagram of the model (6) for $c = 0.2$ and $r = \frac{2}{1-c} = 2.5$ with initial values 1.01 is given in Figure 1, which shows that the equilibrium point 1 is asymptotically stable. By Theorem 2.1, we can also obtain that the equilibrium point 1 is non-hyperbolic and local asymptotically stable.

Flip bifurcation diagram of the model (6) in (r, x) plane for $c = 0.2$ with initial values 1.01 is given in Figure 2, which shows that there is the stable equilibrium point 1 for $r \in (0, 2.5]$, and the equilibrium point 1 loses its stability as r increases. Flip bifurcation occurs at $r = 2.5$. Then there appears to be an unending sequence of the flip bifurcations until chaos as r increases. One can also see that the chaotic behaviour suddenly disappears at $r = 4.157$. In other words, the chaotic behaviour results in the prey population to die out. Maximum Lyapunov exponents diagram corresponding to Figure 2 is given in Figure 3.

Take $c = 0.3$ and $r = 2$. By simple calculations, one can obtain that $r(1 - c) = 1.4 < 2$ and $x_c = 1.366$. By the Theorem 2.2, the basin of the equilibrium point 1 is $(0.3, 1.366)$. Take initial values 0.299, 0.301, 1.365, 1.367, respectively. From Figure 4, we can observe that the equilibrium point 1 is stable when initial values are 0.299 (red curve), 1.367 (yellow

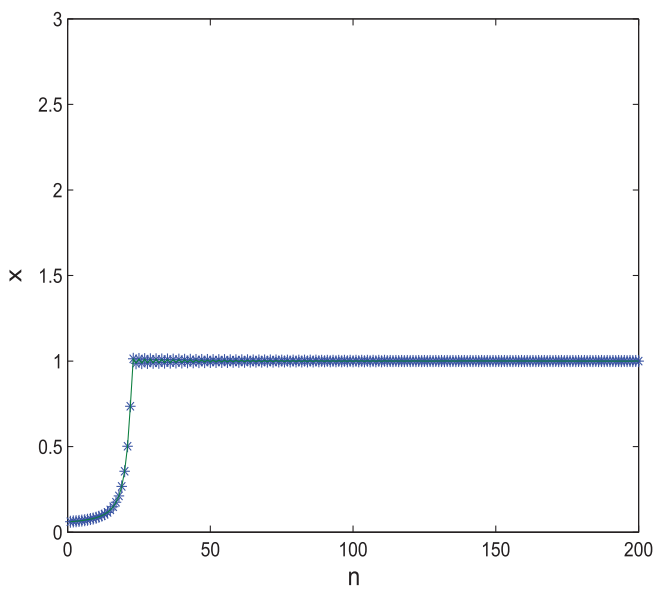


Figure 1. Time sequence diagram of the model (6) with $c = 0.2$ and $r = 2.5$.

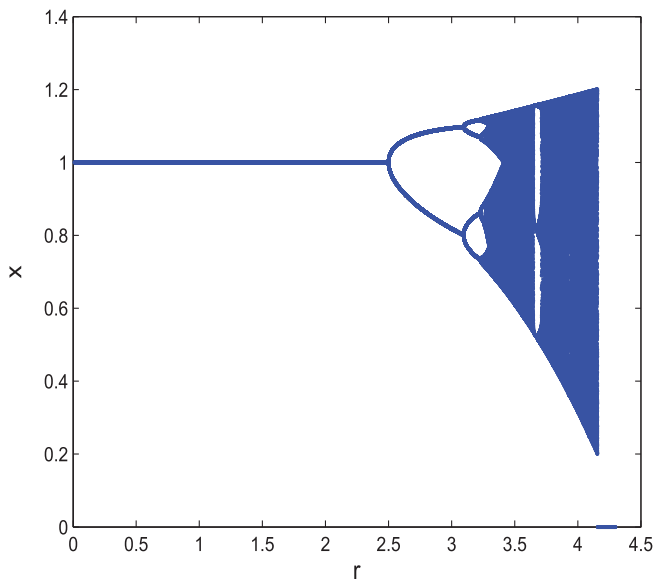


Figure 2. Bifurcation diagram of the model (6) with $c = 0.2$ and $r \in (0, 4.3)$.

curve) and unstable when initial values are 0.301 (blue curve), 1.365 (green curve). Figure 4 verifies the correctness of Theorem 2.2.

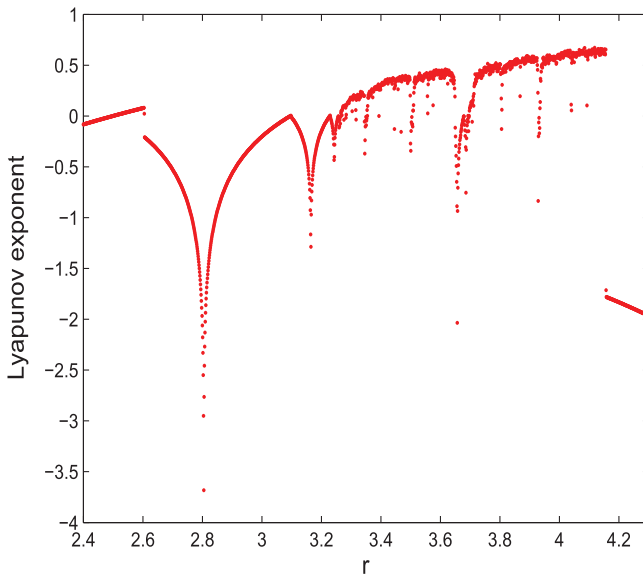


Figure 3. Lyapunov exponents corresponding to Figure 2 for $r \in [2.4, 4.3]$.

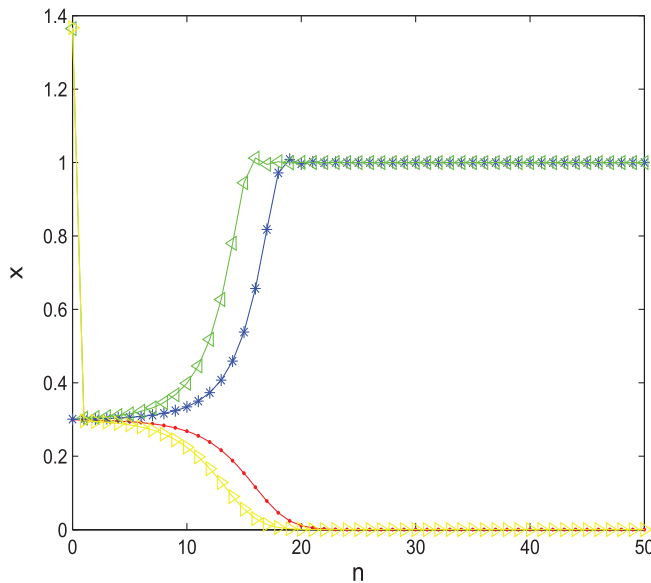


Figure 4. Trajectory diagram of the model (6) with $r = 2$ and $c = 0.3$.

7.2. Numerical simulations on stability and codimension-one bifurcations of the equilibrium points

Trajectory diagram of the model (5) in (n, x, y) for $c = 0.2$, $a = 0.8$ and $r = 2$ with initial values $(0.04, 0.05)$ is given in Figure 5, which shows that the trajectory tends to the equilibrium point $E_0(0, 0)$, i.e. the populations will become ultimate extinction.

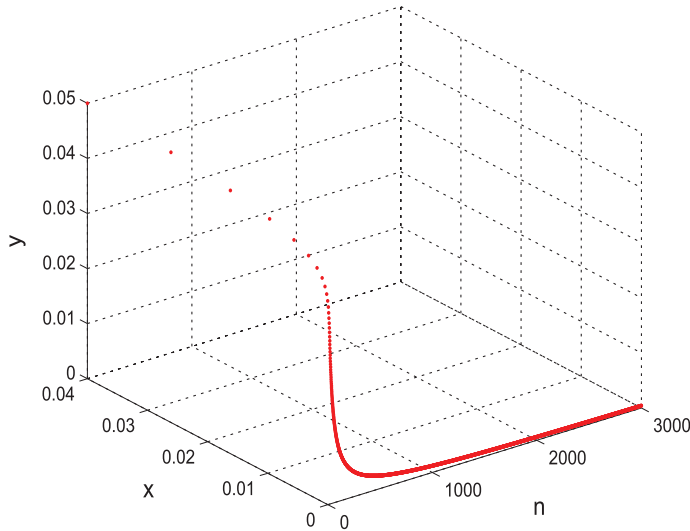


Figure 5. Trajectory diagram of the model (5) with $c = 0.2$, $a = 0.8$ and $r = 2$.

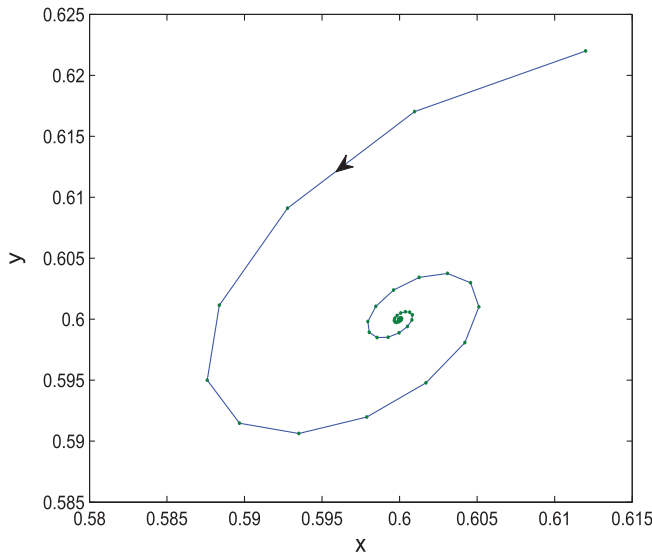


Figure 6. Phase portrait of the model (5) with $c = 0.2$, $a = 0.8$ and $r = 3$ and initial values $(0.612, 0.622)$.

Take $c = 0.2$, $a = 0.8$ and $r = 3$. By simple computations, we can obtain that $x_3^* = y_3^* = 0.600$, $\frac{a}{r} = 0.2667$, $c_1 = 0.1415$, $\frac{(a-1)(1-ac)}{a} = -0.21$. By the Theorem 3.1, the positive equilibrium point $(0.600, 0.600)$ is a stable focus. The phase portrait of the model (5) for $c = 0.2$, $a = 0.8$ and $r = 3$ with initial values $(0.612, 0.622)$ is given in Figure 6, which shows that the trajectory tends to the positive point $(0.600, 0.600)$. Phase portraits are given in Figure 7, which shows that the red curves tend to the equilibrium point $(0, 0)$

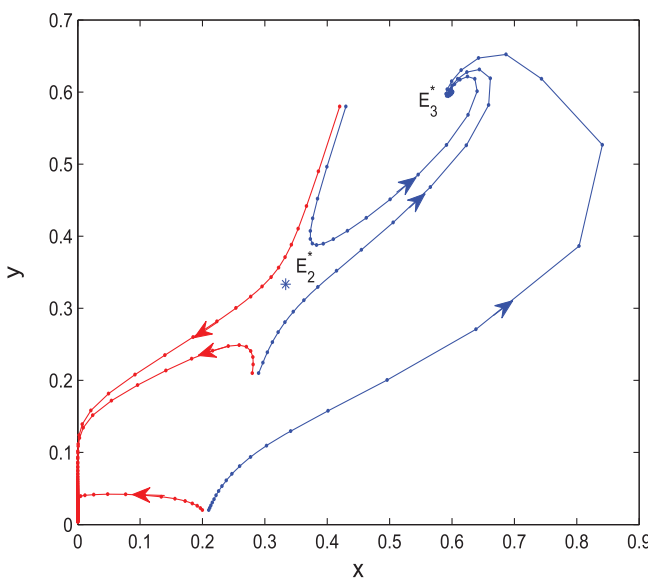


Figure 7. Phase portraits of the model (5) with $c = 0.2, a = 0.8$ and $r = 3$.

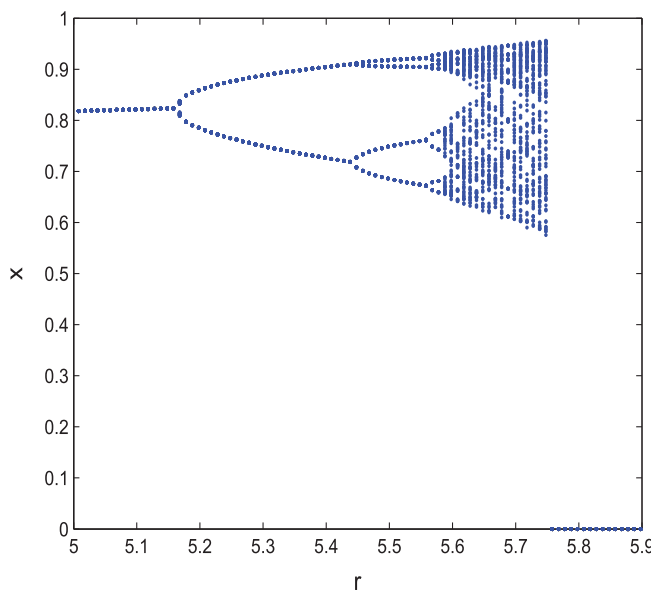


Figure 8. Flip bifurcation diagram of x population for the model (5) with $c = 0.1, a = 0.8$.

and the blue curves tend to the equilibrium point E_3^* . One can also see that the equilibrium point E_2^* is unstable.

Take $c = 0.1$ and $a = 0.8$. By some computations, we can obtain that the bifurcation critical parameter value $r_1 = 5.1583, \tilde{q} = (-1.3411, 0.6589)^T, \tilde{p} = (-0.9829, -0.4829)^T$ and the normal form coefficient $d = 58.9667 > 0$. From the Theorem 4.1, the flip

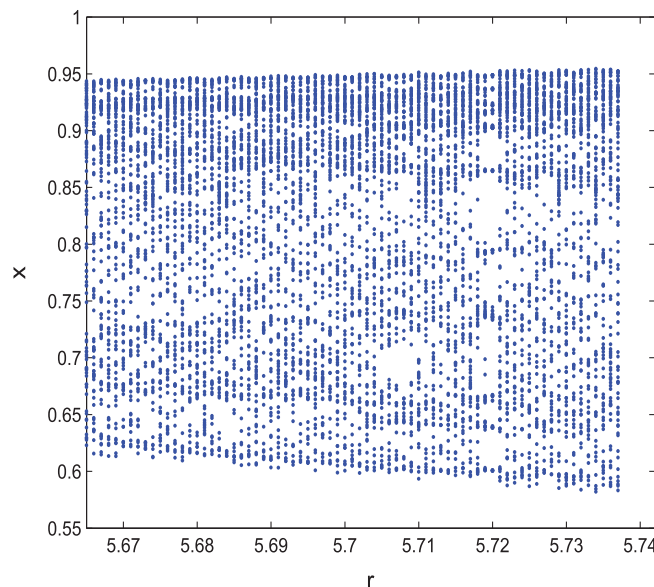


Figure 9. Local amplification of Figure 8.

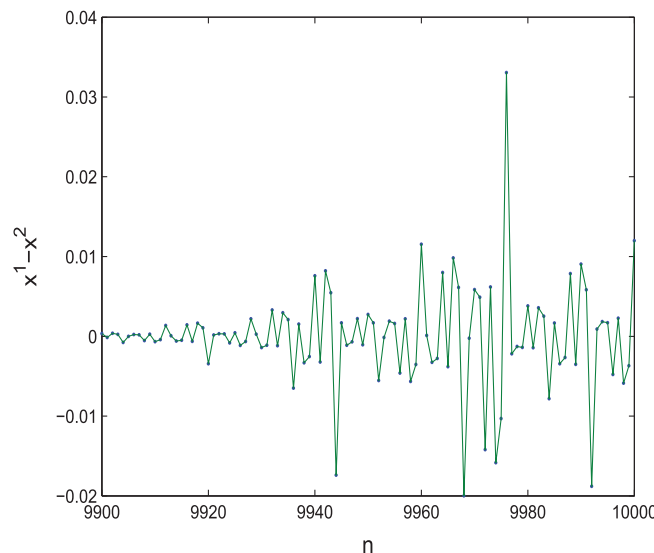


Figure 10. Error diagram of the prey population for the model (5) with $r = 5.730$.

bifurcation of the model (5) at $r = r_1$ is supercritical and the period-doubling cycle is stable. Flip bifurcation diagram of the model (5) in (r, x) plane for $c = 0.1$ and $a = 0.8$ with initial values $(0.8335, 0.8135)$ is given in Figure 8, which shows that there is a stable equilibrium point $E_3^*(x_3^*, y_3^*)$ for $r \in (5, 5.1583)$, and the equilibrium point $E_3^*(x_3^*, y_3^*)$ loses its stability as r increases. Flip bifurcation emerges from the equilibrium point $(0.8235, 0.8235)$ with $r = 5.1583$. Then there appears to be an unending sequence of flip bifurcations until chaos

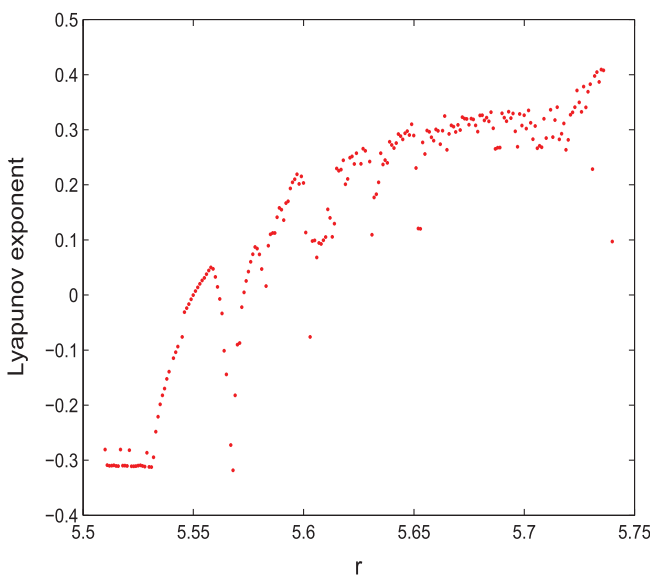


Figure 11. Lyapunov exponents corresponding to Figure 8.

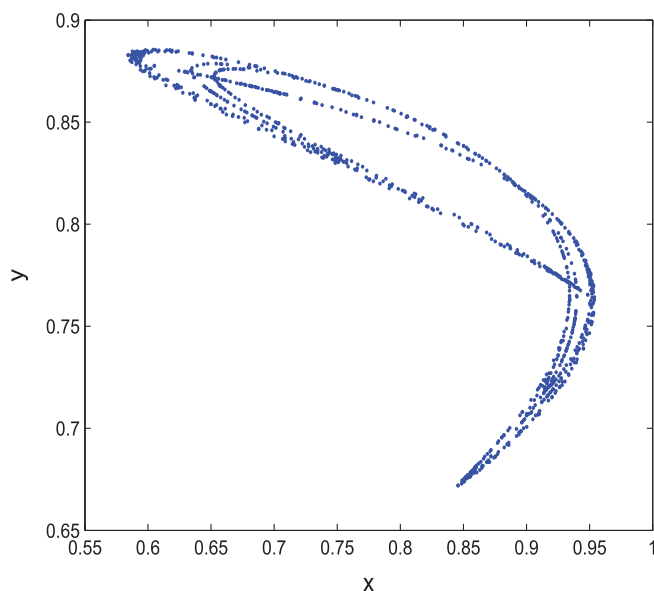


Figure 12. Chaotic attractors of the model (5) with $r = 5.730$.

as r increases. The chaotic behaviour suddenly disappear at $r = 5.7372$. Figure 9 is the local amplification of Figure 8 for $r \in [5.6651, 5.7372]$. Sensitivity of the model trajectories for $r = 5.730$ to the initial values is shown in Figure 10. For that purpose, we consider the error $\Delta x = x^1 - x^2$, where x^1 and x^2 are the solutions of the model (5) with initial values $(0.833, 0.833)$ and $(0.834, 0.833)$ respectively. From the Figure 10, one can see that

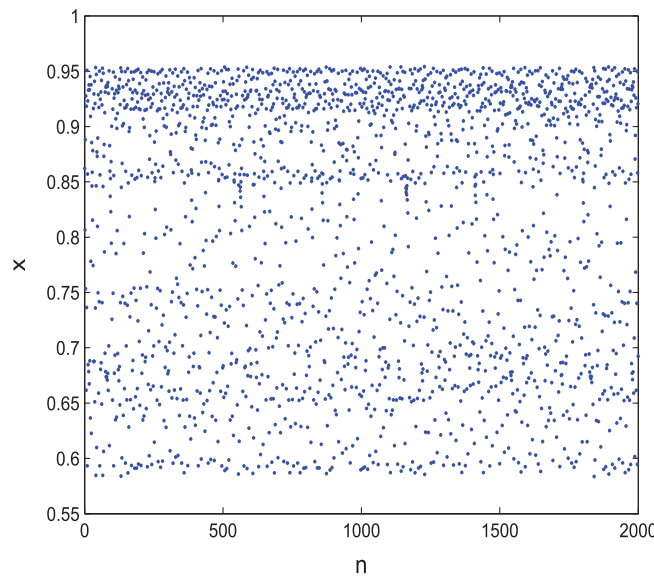


Figure 13. Time sequence diagram of the prey population for the model (5) with $r = 5.730$.

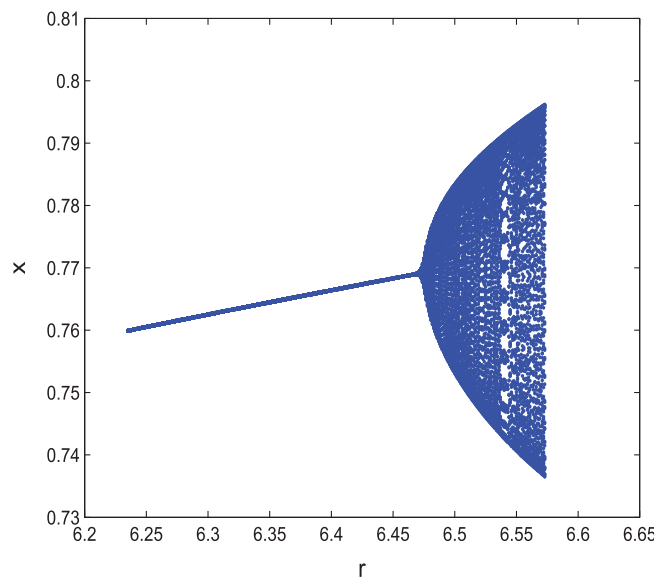


Figure 14. Bifurcation diagram of the prey population for the model (5) with $c = 0.1$, $a = 1.3$ and $r \in [6.235, 6.575]$.

whatever initial error between two trajectories is negligible, but the error increases in the subsequent time. This phenomena ensure the chaotic nature of the model. The Lyapunov exponents diagram corresponding to Figure 8 is given in Figure 11, which shows that the Lyapunov exponents always are positive for $r \in [5.6651, 5.7372]$. This also ensures the chaotic nature. The chaotic attractor at $r = 5.730$ is exhibited in Figure 12. Figure 13

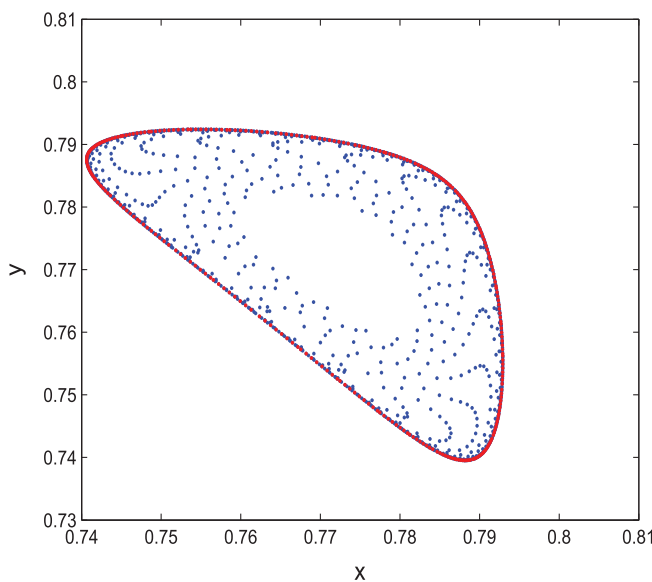


Figure 15. Phase portraits for the model (5) with $c = 0.1$, $a = 1.3$ and 6.475 .

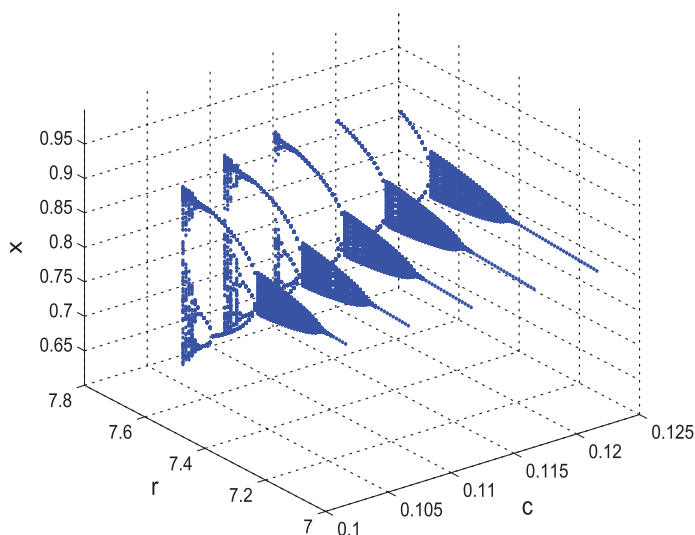


Figure 16. Three dimensions bifurcation diagram for the model (5) with $a = 1.24$, $c \in [0.104, 0.124]$ and $r \in [7.10, 7.75]$.

gives time sequence diagram of the prey population for the model (5) with $r = 5.730$ and shows the chaotic nature. From Figure 8, one can know that the appropriate growth rate can stabilize the model, but the high growth rate may destabilize the stable model into more complex dynamic. From the ecological point of view, the reason is that a population could increase over carrying capacity with high growth rate and then lose its stability. Furthermore, we can also see that the chaotic behaviour leads to the population extinction.

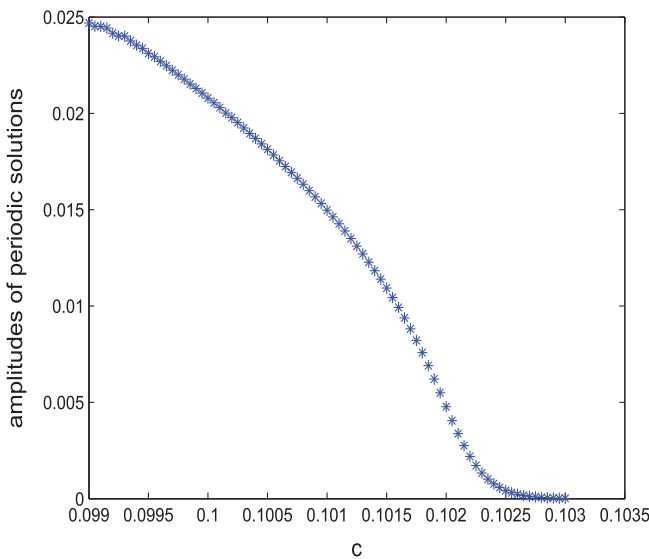


Figure 17. Amplitudes of periodic solutions for the prey population with c varying.

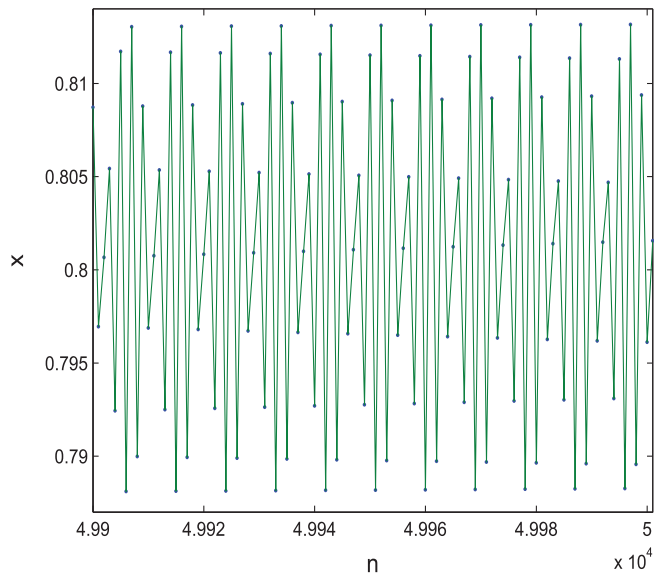


Figure 18. Periodic solutions for the prey population with $c = 0.099$.

Take $c = 0.1$ and $a = 1.3$. By some computations, we can obtain that the bifurcation critical parameter value $r_2 = 6.4751$, $\theta_0 = 2.2043$, $\hat{q} = (1, -0.5920 - 0.8060i)^T$, $\hat{p} = (0.5000 - 0.3672i, -0.6204i)^T$, $\frac{\delta(r(c+1)-a+\delta)}{r}|_{r=r_2} = 6.3678 \neq 4, 6$ and the normal form coefficient $b = -162.72 - 273.85i$. From the Theorem 4.2, the Neimark–Sacker bifurcation for the model (5) at $r = r_2$ is supercritical and the closed invariant curve bifurcating from the equilibrium point $E_3^*(0.772, 0.772)$ is stable. Bifurcation diagram of the model (5)

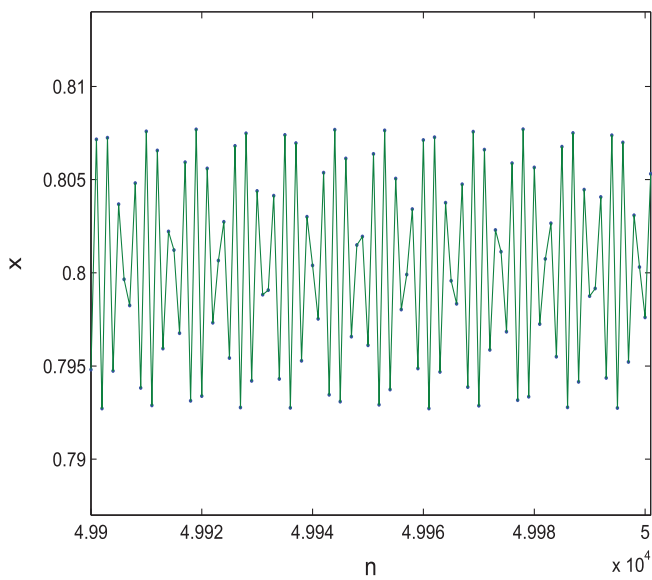


Figure 19. Periodic solutions for the prey population with $c = 0.101$.

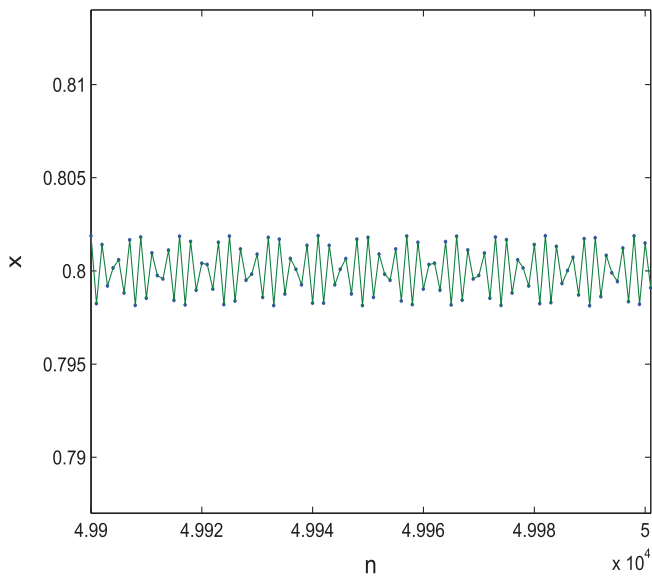


Figure 20. Periodic solutions for the prey population with $c = 0.102$.

in (r, x) is given in Figure 14 for $c = 0.1$, $a = 1.3$ and $r \in [6.235, 6.575]$ with initial values $(0.762, 0.782)$. Figure 14 shows that the Neimark–Sacker bifurcation occurs at the equilibrium point $E_3^*(0.772, 0.772)$ and $r = 6.4751$. The closed invariant curve bifurcating from the equilibrium point $E_3^*(0.772, 0.772)$ is shown in Figure 15 (red curve).

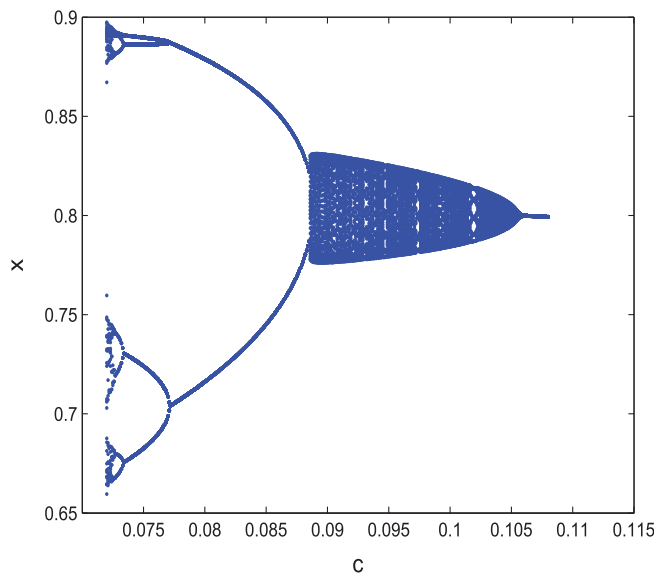


Figure 21. Bifurcation diagram of the prey population for the model (5) with $r = 7.2$, $a = 1.25$ and $c \in [0.072, 0.108]$.

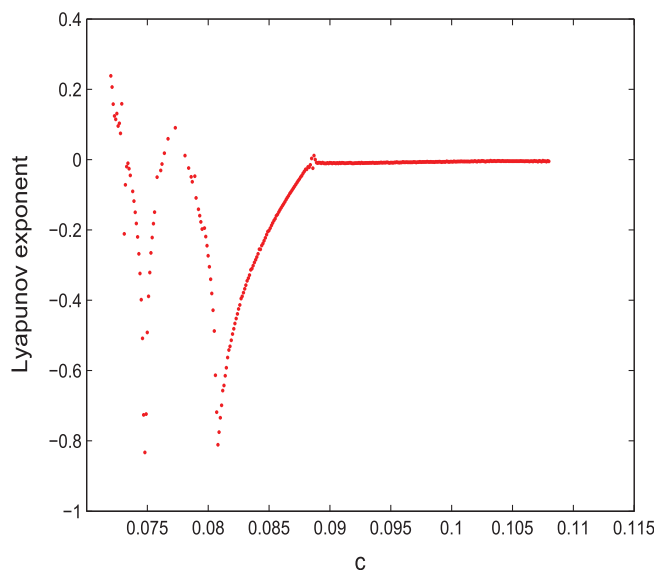


Figure 22. Lyapunov exponents corresponding to Figure 21.

Take $a = 1.24$, $c \in [0.104, 0.124]$ and $r \in [7.10, 7.75]$. By sample computations, we can obtain that if $c = 0.11708$ and $r = 7.4986$, then $r - \frac{a}{(1-\sqrt{c})^2} = 4.6099 > 0$, $c_1 = \frac{a}{r} = \frac{(a-1)(1-ac)}{a} = 0.1654$, $\tilde{c} = -72.8192 < 0$ and $\tilde{c} + \tilde{d} = 240.2946 > 0$. By Theorem 5.1, the codimension-two bifurcation with 1:2 resonance occurs at $(0.8066, 0.8066)$. Three dimensions bifurcation diagram is shown in Figure 16.

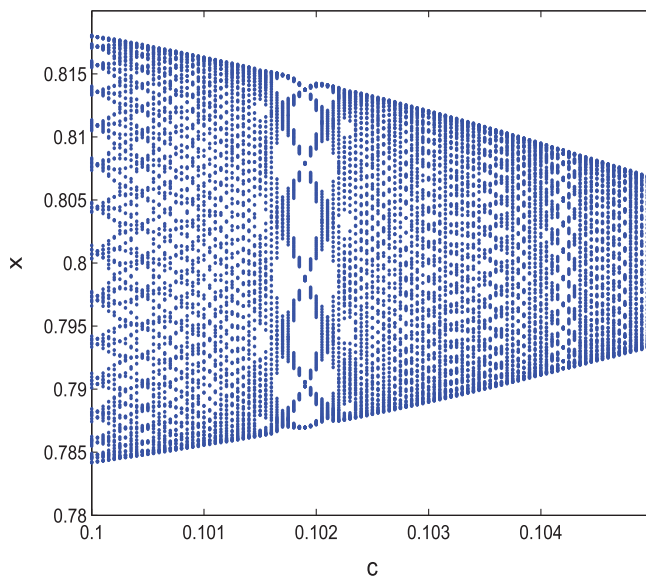


Figure 23. Local amplification of Figure 21 for $c \in [0.1, 0.105]$.

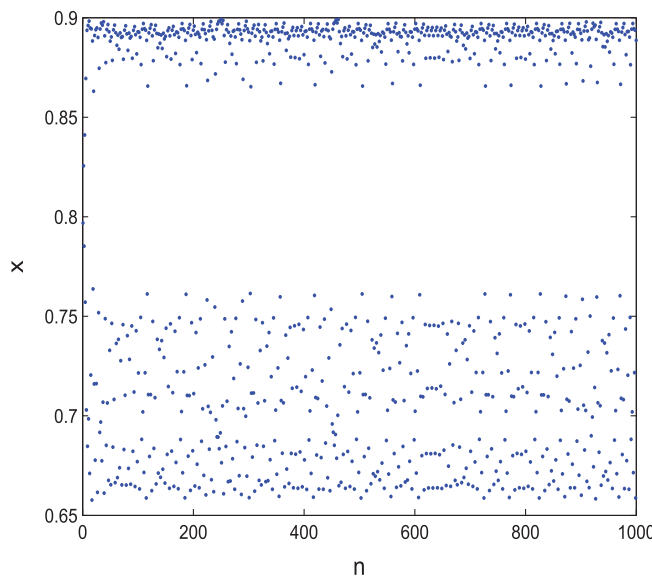


Figure 24. Time sequence diagram of the prey population for $c = 0.072$ in Figure 21.

7.3. Impact of the Allee effect on the amplitudes of periodic solutions

In this subsection, we analyze the impact of the Allee effect on the amplitudes of periodic solutions. Take $r = 7.164$, $a = 1.25$ and $c \in [0.0990, 0.103]$. From Figure 17, one can see that the amplitudes of periodic solutions are decreasing for $c \in [0.0990, 0.103]$. The periodic solutions for the prey population are shown by Figures 18–20 with $c =$

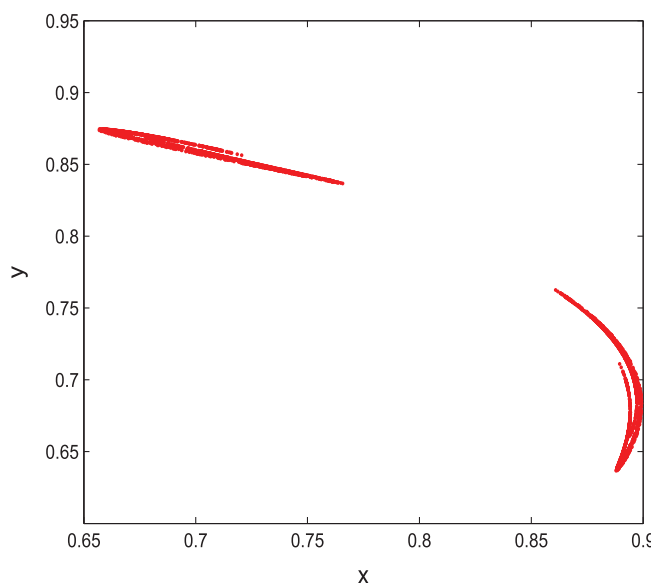


Figure 25. Chaotic attractors for $c = 0.072$ in Figure 21.

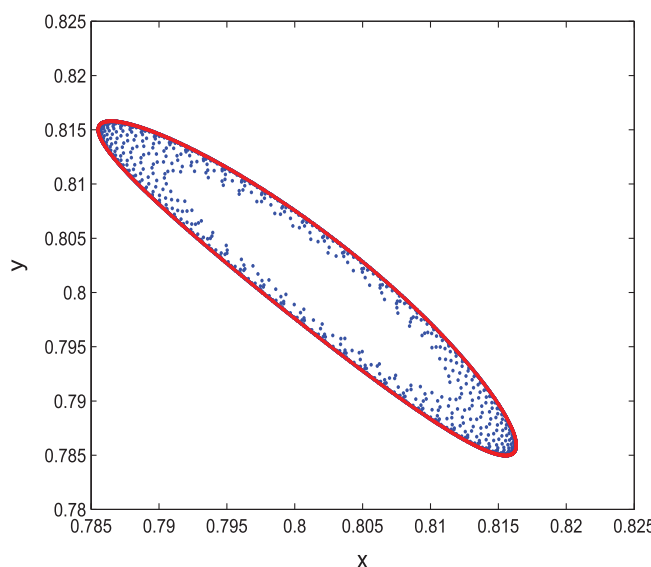


Figure 26. Phase portraits for $c = 0.101$ in Figure 21.

0.099, 0.101, 0.102, respectively. From the population ecological point of view, the Allee effect impacts the amplitude of persistent survival for the population. In other words, with appropriate intrinsic growth rate, the lower Allee effect constant will benefit to the populations to have a higher recovery and to be more prone to survival.

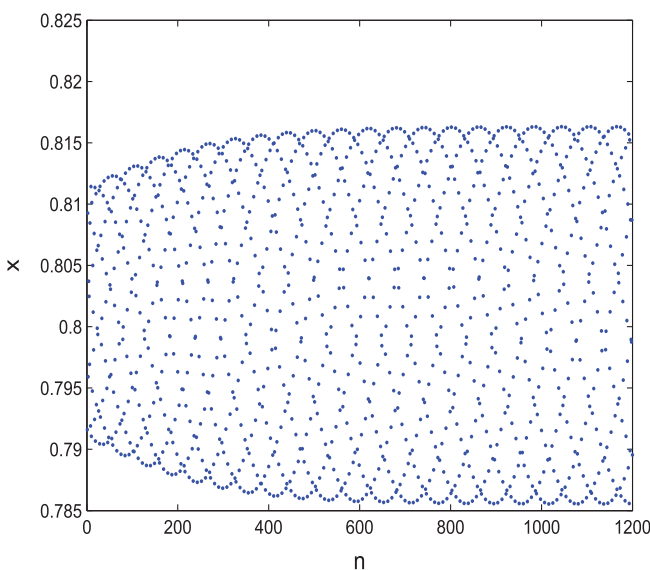


Figure 27. Time sequence diagram of the prey population for $c = 0.101$ in Figure 21.

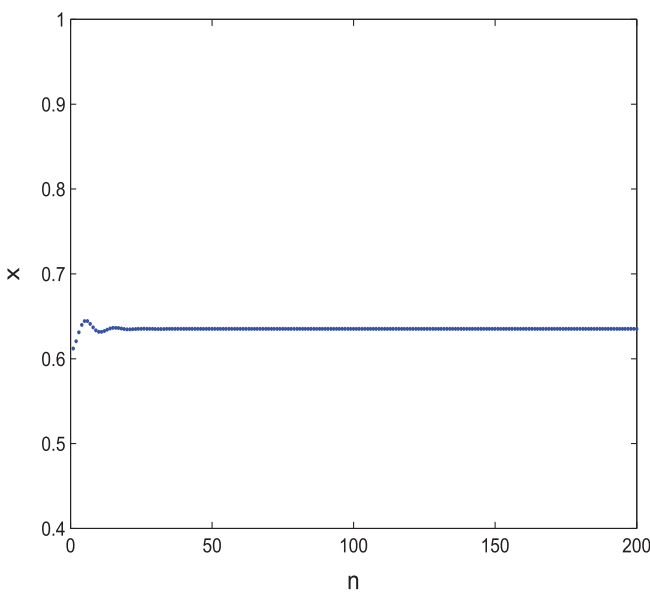


Figure 28. Phase portraits for $c = 0.107$ in Figure 21.

7.4. Further numerical simulations for the model (5)

Take $r = 7.2$, $a = 1.25$ and $c \in [0.072, 0.108]$. From Figure 21, we can see that $c = 0.1055$ and $c = 0.0888$ are the critical values when the model (5) undergoes the Neimark-Sacker bifurcation and the flip bifurcation, respectively. As c decreases beyond $c = 0.1055$, the positive equilibrium point E_3^* loses its stability and closed invariant curve occurs.

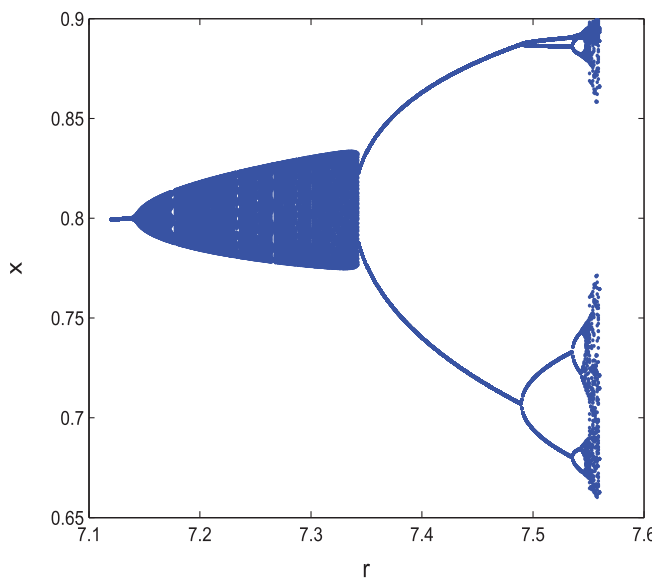


Figure 29. Bifurcation diagram of the prey population for the model (5) with $c = 0.1$, $a = 1.25$ and $r \in [7.121, 7.562]$.

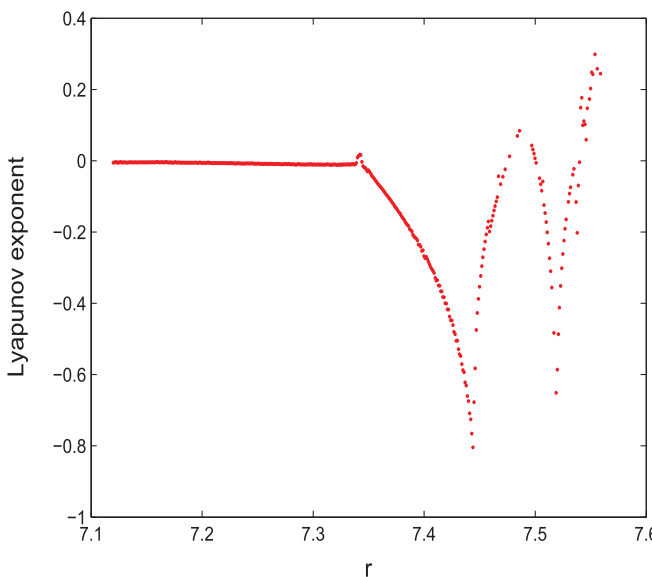


Figure 30. Lyapunov exponents corresponding to Figure 29.

As c further decreases beyond 0.0888, the inverse period doubling bifurcates to chaos with complex periodic windows, including inverse period-4 doubling bifurcation for $c \in [0.0734, 0.0771]$ and the chaotic behaviour suddenly appears at $c = 0.0724$. Lyapunov exponents diagram corresponding to Figure 21 is given in Figure 22, which shows that the maximum Lyapunov exponents are greater than 0 for $c \in [0.072, 0.0724]$. Figure 23

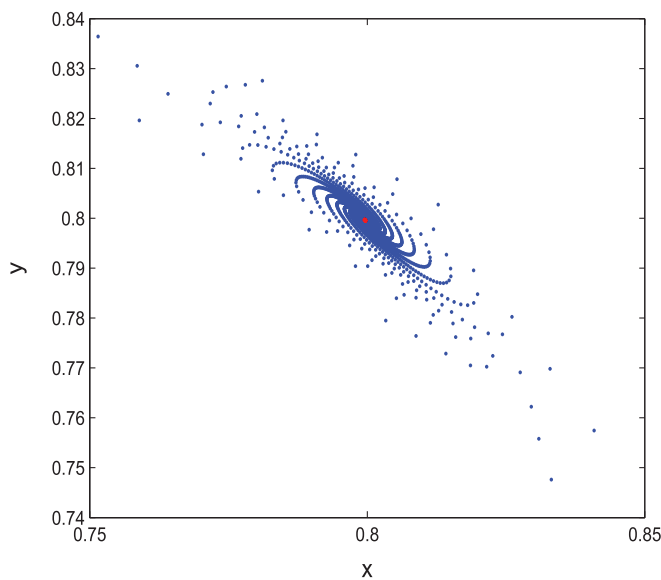


Figure 31. Phase portraits for the model (5) with $r = 7.129$.

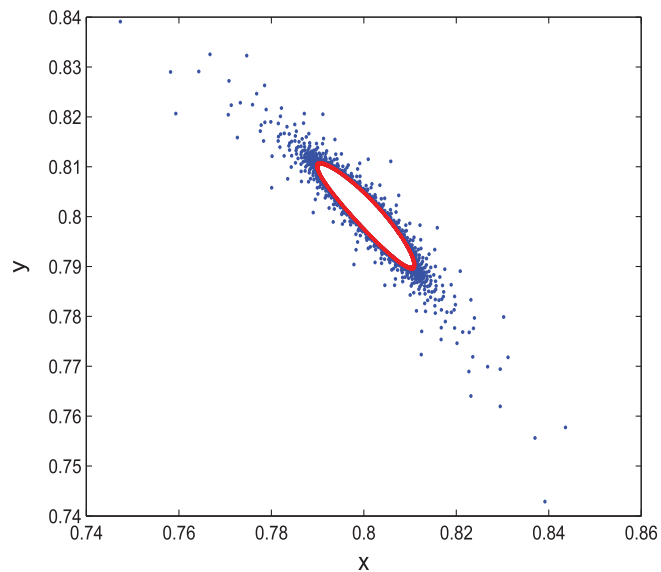


Figure 32. Phase portraits for the model (5) with $r = 7.164$.

is the local amplification of Figure 21 for $c \in [0.1, 0.105]$. Time sequence diagram of the prey population for the model (5) is given in Figure 24 for $c = 0.072$. The chaotic attractors (two-coexisting chaotic sets) are shown in Figure 25 for $c = 0.072$. The phase portraits diagram for $c = 0.101$ is given in Figure 26, which shows that closed invariant curve (red curve) is stable. Time sequence diagram of the prey population for the model (5) with $c = 0.101$ is given in Figure 27. Phase portraits diagram for $c = 0.107$ is given

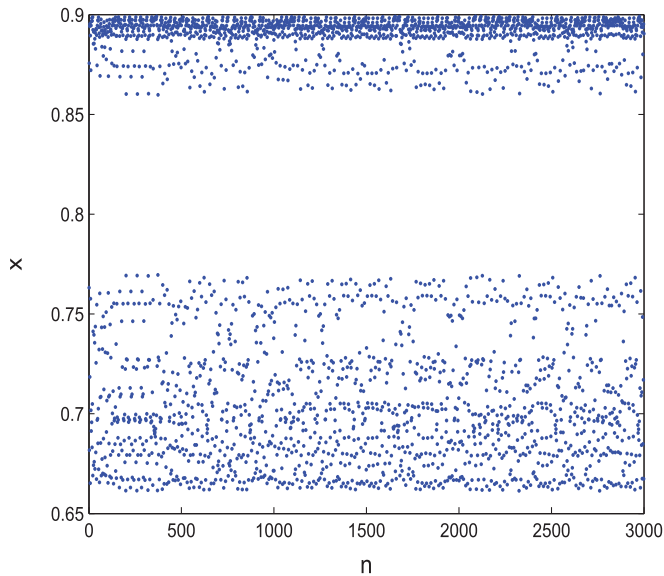


Figure 33. Time sequence diagram for the model (5) with $r = 7.556$.

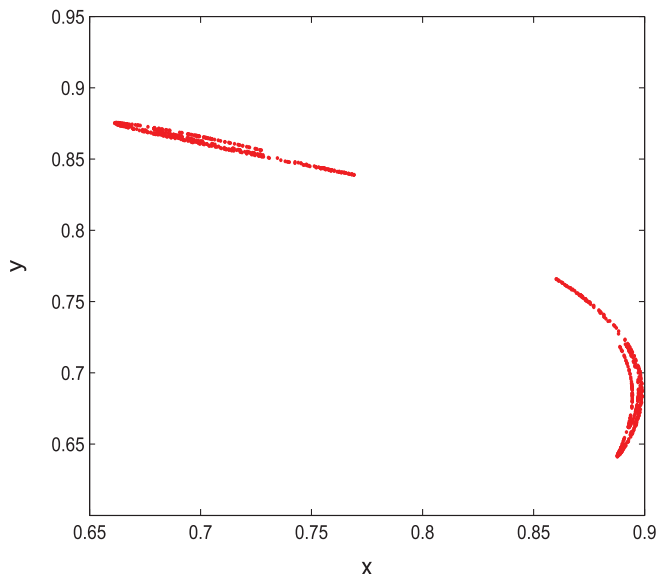


Figure 34. Chaotic attractors for the model (5) with $r = 7.556$.

in Figure 28, which shows that the positive equilibrium E_3^* (red dot) is stable. We can find that the equilibrium point E_3^* is asymptotically stable for the Allee effect parameter $c \in [0.1056, 0.1389]$. According to Figure 21, one can obtain that with high intrinsic growth rate, the appropriate Allee effect constant can stabilize the model (5), but the low Allee effect may destabilize the stable model (5) into more complex dynamic.



Take $c = 0.1$, $a = 1.25$ and $r \in [7.121, 7.562]$. Bifurcation diagram is shown in Figure 29 with $c = 0.1$, $a = 1.25$ and $r \in [7.121, 7.562]$. Lyapunov exponents diagram corresponding to Figure 29 is given in Figure 30. The positive equilibrium point suddenly loses its stability and the closed invariant curve appears for $r = 7.1432$, i.e. the Neimark–Sacker bifurcation occurs. The closed invariant curve suddenly disappears and bifurcates to stable period-2 solutions for $r = 7.3384$, i.e. the flip bifurcation occurs. The period doubling bifurcates to chaos with complex periodic windows, including period-8 doubling bifurcation to chaos and the chaotic behaviour suddenly appear for $r = 7.5461$. In Figure 31, phase portraits diagram shows that the positive equilibrium point (red dot) is stable for $r = 7.129$. In Figure 32, phase portraits diagram shows that the closed invariant curve (red curve) is stable for $r = 7.164$. The chaotic behaviours and the chaotic attractors (two-coexisting chaotic sets) for $r = 7.556$ are shown in Figures 33 and 34, respectively.

8. Conclusion and discussion

The Allee effect is considered as an important ecological phenomenon. With a population subject to the Allee effect, it is well known that there exists a critical population level below which the population will go extinct [10]. Consequently, studying population interactions involving Allee effects becomes an important subject of contemporary research.

In this paper, we first discuss the prey population that follows the classical discrete logistic model and is also subject to the Allee effect. It is proved that there exists a threshold r_0 in terms of the Allee threshold c . The flip bifurcation occurs for the equilibrium point 1 at $r = r_0$. By numerical simulations, we can see that the prey population undergoes a cascade of period-doubling bifurcations and eventually be chaotic if r is increased further. Theorem 2.2 gives the basins of attraction of the equilibrium points, especially the basin of 0 when r is large which makes the map f possess the chaotic behaviour. The previous works with Allee effects (see [9,17,18]) hardly discussed these. The basins of attraction show that the prey population either goes to extinction or stabilizes at the carrying capacity if its intrinsic growth rate r is less than r_0 .

For the predator–prey model, we research the stability of the equilibrium points. Almost all papers do not further research the stability of the extinction equilibrium point $E_0(0, 0)$ which is non-hyperbolic (see [6–8,36,39]). The extinction equilibrium point $E_0(0, 0)$ is non-hyperbolic and locally asymptotically stable in $\{(x, y) | x \geq 0, y \geq 0\}$.

The equilibrium point $E_1(1, 0)$ is unstable. Due to the Allee effect, for a larger intrinsic growth rate, there are two positive equilibrium points. We prove that the smaller equilibrium point is always unstable, and the larger equilibrium point can be either an attractor or a repeller surrounded by a invariant curve. While r crosses $\frac{a}{(1-\sqrt{c})^2}$ from right to left, the two existence equilibrium points collide, forming an equilibrium point, and disappear. It shows that the model (5) undergoes fold bifurcation due to Allee effects. The extinction equilibrium point $(0, 0)$ for the model (2) is always unstable and the unique existence equilibrium point may be asymptotically stable. However, Theorem 3.1 implies that the model (5) possesses the bistability phenomenon, where both the extinction equilibrium point and the existence equilibrium point are stable. By using the center manifold theorem and the bifurcation theory, we obtain that the model (5) exists the flip bifurcation and the Neimark–Sacker bifurcation under some conditions at the larger positive equilibrium point $E_3(x_3^*, y_3^*)$ which are given in Theorem 4.1 and Theorem 4.2. The model (5) only exhibits

a supercritical flip bifurcation and it is possible for the model to exhibit a supercritical or subcritical Neimark–Sacker bifurcation at the larger positive equilibrium point $E_3(x_3^*, y_3^*)$, while other predator–prey models with the Allee effect only give a general criterion for bifurcation direction (see [6–8,36,39]). To the best of our knowledge, literatures about the discrete predator–prey model with Allee effects rarely discuss the codimension-two bifurcations at the positive equilibrium point (see [6–8,36,39]). In this paper, we derive critical conditions and the normal coefficients of codimension-two bifurcations with 1:2 resonance. Chaos in the sense of Marotto is proved by analytical methods. However, other predator–prey models with Allee effects only illustrated the chaos by the numerical simulation (see [6–8,36,39]).

Numerical simulations including bifurcation diagrams, phase portraits, sensitivity dependence on the initial values, Lyapunov exponents display rich and complex dynamical behaviour. From Figure 8, one can know that the appropriate intrinsic growth rate can stabilize the model (5), but the high intrinsic growth rate may destabilize the stable model (5) into more complex dynamic. From the ecological point of view, the reason is that a population could increase over carrying capacity with high intrinsic growth rate and then lose its stability. Furthermore, we also can see that the chaotic behaviour leads to the population extinction. Figures 17–20 show that the Allee effect impacts the amplitude of persistent survival for the prey population. With appropriate intrinsic growth rate, the lower Allee effect constant will benefit to the populations to have a higher recovery and to be more prone to survival. According to Figure 21, one can obtain that with higher intrinsic growth rate, the appropriate Allee effect constant can stabilize the model (5), but the lower Allee effect may destabilize the stable model (5) into more complex dynamic.

Acknowledgements

Authors would like to thank the anonymous referees for their helpful comments and suggestions which led to an improvement of original manuscript.

Disclosure statement

No potential conflict of interest was reported by the authors.

Funding

The work is partially supported by the National Natural Science Foundation of China [grant number 11571170], [grant number 61174155], [grant number 31570417]; the Natural Science Foundation of Anhui Province of China [grant number 1608085MA14], [grant number 1608085MC63]; the Key Project of Natural Science Research of Anhui Higher Education Institutions of China [grant number KJ2015A152].

References

- [1] W. Allee, *Animal Aggregations. A Study in General Sociology*, University of Chicago Press, Chicago, 1931.
- [2] L. Allen, *An Introduction to Mathematical Biology*, Prentice Hall, Upper Saddle River, NJ, 2007.
- [3] M. Andrew, D. Brian, M. Andrew, and M. John, *The evidence for Allee effects*, Popul. Ecol. 52 (2009), pp. 341–354.



- [4] A.D. Bazykin, *Nonlinear Dynamics of Interacting Populations*, World Scientific, Singapore, 1998.
- [5] D. Boukal and L. Berec, *Single-species models of the Allee effect: Extinction boundaries, sex ratios and mate encounters*, Trends Ecol. Evol. 218 (2002), pp. 317–394.
- [6] C. Celik and O. Duman, *Allee effect in a discrete-time predator-prey system*, Chaos Solitons Fractals 40 (2009), pp. 1956–1962.
- [7] X. Chen, X. Fu and Z. Jing, *Dynamics in a discrete-time predator-prey system with Allee effect*, Acta Math. Appl. Sin. 29 (2013), pp. 143–164.
- [8] L. Cheng and H. Cao, *Bifurcation analysis of a discrete-time ratio-dependent predator-prey model with Allee effect*, Commun. Nonlinear Sci. Numer. Simulat. 38 (2016), pp. 288–302.
- [9] Y. Chow and S. Jang, *Allee effects in a Ricker-type predator-prey system*, J. Differ. Equ. Appl. 20 (2014), pp. 1350–1371.
- [10] F. Courchamp, L. Berec, and J. Gascoigne, *Allee Effects in Ecology and Conservation*, Oxford University Press, New York, 2008.
- [11] F. Courchamp, J. Clutton-Brock, and B. Grenfell, *Inverse density dependence and the Allee effect*, J. Theor. Biol. 14 (1999), pp. 405–410.
- [12] F. Courchamp, B. Grenfell, and T. Clutton-Brock, *Impact of natural enemies on obligately cooperatively breeders*, Oikos 91 (2000), pp. 311–322.
- [13] F. Dannan, S. Elaydi, and V. Ponomarenko, *Stability of hyperbolic and nonhyperbolic fixed points of one-dimensional maps*, J. Differ. Equ. Appl. 9 (2003), pp. 449–457.
- [14] S. Elaydi, *An Introduction to Difference Equations*, 3rd ed., Springer, New York, 2005.
- [15] J. Ferdy, F. Austerlitz, J. Moret, P. Gouyon, and B. Godelle, *Pollinator-induced density dependence in deceptive species*, Oikos 87 (1999), pp. 547–560.
- [16] K. Gopalsamy, *Stability and Oscillation in Delay Differential Equation of Population Dynamics*, Kluwer Academic, Dordrecht, 1992.
- [17] S. Jang, *Allee effects in a discrete-time host-parasitoid model*, J. Differ. Equ. Appl. 12 (2006), pp. 165–181.
- [18] S. Jang, *Allee effect in a discrete-time host-parasitoid model with stage structure in the host*, Discrete Contin. Dyn. Syst. Ser. B 8 (2007), pp. 145–159.
- [19] Y. Kang, *Dynamics of generalized Ricker-Beverton-Holt competition model subject to Allee effects*, J. Differ. Equ. Appl. 22 (2016), pp. 687–723.
- [20] M. Kuussaari, I. Saccheri, M. Camara, and I. Hanski, *Allee effect and population dynamics in the Glanville fritillary butterfly*, Oikos 82 (1998), pp. 384–392.
- [21] Yu.A. Kuznetsov, *Elements of Applied Bifurcation Theory*, 2nd ed., Springer, New York, 2004.
- [22] Yu.A. Kuznetsov and H. Meijer, *Numerical normal forms for codim 2 bifurcations offixed points with at most two critical eigenvalues*, SIAM J. Sci. Comput. 26 (2005), pp. 1932–1954.
- [23] B. Li and Z. He, *Bifurcations and chaos in a two-dimensional discrete Hindmarsh-Rose model*, Nonlinear Dyn. 76 (2014), pp. 697–715.
- [24] B. Li and Z. He, *1:2 and 1:4 resonances in a two-dimensional discrete Hindmarsh-Rose model*, Nonlinear Dyn. 79 (2015), pp. 705–720.
- [25] T. Li and J. Yorke, *Period three implies chaos*, Amer. Math. Monthly 82 (1975), pp. 985–992.
- [26] X. Liu and Y. Lou, *Global dynamics of a predator-prey model*, J. Math. Anal. Appl. 371 (2010), pp. 323–340.
- [27] F. Marotto, *Snap-back repellers imply chaos in R^n* , J. Math. Anal. Appl. 63 (1978), pp. 199–223.
- [28] F. Marotto, *On redefining a snap-back repeller*, Chaos Solitons Fractals 25 (2005), pp. 25–28.
- [29] M. McCarthy, *The Allee effect, finding mates and theoretical models*, Ecol. Model. 103 (1997), pp. 99–102.
- [30] J. Murray, *Mathematical Biology*, Springer, New York, 1993.
- [31] S. Oseledec, *A multiplicative ergodic theorem: Lyapunov characteristic numbers for dynamical systems*, Trans. Moscow Math. Soc. 19 (1968), pp. 197–231.
- [32] S.J. Schreiber, *Chaos and population disappearances in simple ecological models*, J. Math. Biol. 42(3) (2001), pp. 239–260.
- [33] R. Smith, C. Tan, J. Srimani, and A. Pai, *Programmed Allee effect in bacteria causes a tradeoff between population spread and survival*, Proc. Natl. Acad. Sci. 111 (2014), pp. 1969–1974.

- [34] A. Stoner and M. Ray-Culp, *Evidence for Allee effects in an over-harvested marine gastropod: Density-dependent mating and egg production*, Mar. Ecol. Prog. Ser. 202 (2000), pp. 297–302.
- [35] C. Wang and X. Li, *Further investigations into the stability and bifurcation of a discrete predator-prey model*, J. Math. Anal. Appl. 422 (2015), pp. 920–939.
- [36] W. Wang, Y. Zhang, and C. Liu, *Analysis of a discrete-time predator-prey system with Allee effect*, Ecol. Complex. 8 (2011), pp. 81–85.
- [37] S. Wiggins, *Introduction to Applied Nonlinear Dynamical Systems and Chaos*, Springer-Verlag, Berlin, 1990.
- [38] L. Yuan and Q. Yang, *Bifurcation, invariant curve and hybrid control in a discrete-time predator-prey system*, Appl. Math. Model. 39 (2015), pp. 2345–2362.
- [39] L. Zhang, C. Zhang, and M. Zhao, *Dynamic complexities in a discrete predator-prey system with lower critical point for the prey*, Math. Comput. Simulat. 105 (2014), pp. 119–131.